Sedimentary Geology 475 (2025) 106782

Contents lists available at ScienceDirect

Sedimentary Geology

journal homepage: www.elsevier.com/locate/sedgeo

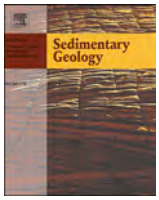

Characterization of *Halimeda* Bioherms of the Pre-Evaporitic Messinian of the Salento Peninsula (Southern Italy)

Chiara Passaseo, Michele Morsilli *

Dipartimento di Fisica e Scienze della Terra, Università di Ferrara, 44122 Ferrara, Italy

ARTICLE INFO

Editor: Dr Basilici Giorgio

Keywords:
Carbonate factories
Upper Miocene
Halimeda
Mediterranean
Nutrients
Internal waves

ABSTRACT

Calcareous green algae bioherms have recently gained significant attention in the scientific community, as they serve as valuable stratigraphic and paleoecological archives, comparable to the most studied coral reefs. Currently, the genus *Halimeda*, which is very abundant in tropical settings and common in temperate ones, contributes significantly to the production of sediments rich in $CaCO_3$. This is due to a rapid calcification process that occurs in its peculiar internal structure. *Halimeda* bioherms represent a key case because of their non-continuous distribution in the stratigraphic record and in the Modern oceans. In fact, the presence of the green alga *Halimeda* is widely documented in present-day reefs throughout the entire tropical belt, although extensive bioherms are limited to areas such as the Indonesian K-Bank, the Caribbean, and particularly along the Australian Great Barrier Reef (GBR), where they reach remarkable extensions exceeding 6000 km^2. Discontinuous distribution is also noted during the Miocene, with *Halimeda* bioherms reported only in three main localities within the Mediterranean basin, all dating to the pre-evaporitic Messinian. In this study, we present data obtained from detailed stratigraphic and sedimentological analyses of two small *Halimeda* bioherms (with a maximum thickness of 5 to 6 m), located in the southernmost portion of the Apulia Carbonate Platform (Salento Peninsula, Italy). Field observations, coupled with thin sections analysis show that despite these two sections being ascribed to different stratigraphic intervals, both record the same facies, with an alternation of shallowing-deepening cycles. While it is documented that different *Halimeda* species currently inhabiting carbonate systems respond variably to factors such as light, temperature, and salinity, the input of large quantities of nutrients via upwelling currents has recently become the most widely accepted hypothesis to support the occurrence of wide bioherms such as along the GBR. We infer that the occurrence of Salento Messinian *Halimeda*-rich facies could be related to upwelling of cool, nutrient-rich waters, possibly enhanced by the occurrence of internal waves (IWs). Such processes are well documented in the Salento Peninsula and in many areas of the Mediterranean throughout the Tortonian and likely still acting during the early Messinian.

1. Introduction

Halimeda (Lamouroux, 1812) is a genus of green calcareous macroalga belonging to the Bryopsidaceae/Halimedaceae family (Hillis-Colinvaux, 1980). It is particularly abundant in some modern marine tropical seas (McNeil et al., 2016, 2021a,b and references therein) and present in temperate ones such as in the Mediterranean Sea (Fornos et al., 1992; Muntaner-Gonzalez et al., 2024), making a significant contribution to the production of $CaCO_3$ sediments (Milliman, 1993; Hillis, 1997; Rees, 2006; Rees et al., 2007; Perry et al., 2016; Castro-Sanguino et al., 2020; McNeil et al., 2021a,b). The substantial contribution to carbonate production is directly related to the peculiar internal structure of the algal segments, which leads to a rapid calcification and a subsequent filling of inter-utricular spaces with aragonite crystals (Wilbur et al., 1969; Hillis-Colinvaux, 1980; Multer, 1988; Drew, 1993; Wizemann et al., 2014). The carbonate production is also influenced by sea-water chemistry, light intensity, and temperature (Ries et al., 2009; Stanley et al., 2010; Stokes et al., 2020; Wei et al., 2022).

Halimeda occurs in various environmental settings from relatively shallow-water, sandy lagoons, usually associated with seagrass and other macroalgae, to wide submerged plateaux or open shelves, to the deepest areas of the photic zone (Drew, 1993; Littler et al., 1985; Hillis-Colinvaux, 1986). Although *Halimeda* occupies a wide bathymetric range (generally from 2 to 150 m) (Multer, 1988), it currently thrives

* Corresponding author.
E-mail address: mrh@unife.it (M. Morsilli).

https://doi.org/10.1016/j.sedgeo.2024.106782
Received 29 August 2024; Received in revised form 10 November 2024; Accepted 15 November 2024
Available online 22 November 2024

under optimal conditions at depths between 20 and 65 m, in euphotic to mesophotic setting, where a balance of light radiance and moderate hydrodynamic energy occurs (McNeil et al., 2016, 2021a,b; Reolid et al., 2024). In this context forms in some cases extensive bioherms from a few tens of meters thick up to more than 140 m or more (Hine et al., 1988; Roberts et al., 1988; McNeil et al., 2016, 2021a,b; Fournier et al., 2024).

The term "*Halimeda* bioherms" was used to describe "mounds that have relief above the sea floor, but do not exhibit a clear framework and contain quite-water characteristic" (Marshall and Davies, 1988). The Holocene *Halimeda* bioherms garnered scientific attention, especially since the 1970s when seismic surveys revealed their topographic surfaces and associated internal structures. Descriptions of these bioherms have been provided from various tropical areas, including the Great Barrier Reef (Davies and Marshall, 1985; Orme, 1985; Drew and Abel, 1988; Marshall and Davies, 1988; Orme and Salama, 1988; Searle and Flood, 1988; Orme and Riding, 1995; McNeil et al., 2016, 2021a,b, 2022; Reolid et al., 2024), Indonesia (K-Bank) (Roberts et al., 1987, 1988; Phipps and Roberts, 1988), the Caribbean (Hine et al., 1988), and India (Rao et al., 1994, 2018).

Despite *Halimeda* having a fossil record dating back to the Upper Cretaceous (Conard and Rioult, 1977; Hillis-Colinvaux, 1980) and possibly to the late Permian (Poncet, 1989), *Halimeda*-rich beds have been described only from few Paleocene and Eocene successions from Egypt, Morocco, Iraq, and Oman (Elliott, 1959; Dragastan and Soliman, 2002; Dragastan and Herbig, 2007). Eocene to early Oligocene abundant *Halimeda*-rich beds are reported from core wells of the Basho Seamount in the Philippine Sea (Takayanagi et al., 2007). These accumulations, however, do not represent real bioherms, but rather structures that cannot be associated with the definition of *Halimeda* bioherms as provided by Marshall and Davies (1988). The largest and oldest bioherms, referred to the early Oligocene, has been described by Fournier et al. (2024) from subsurface data from Palawan offshore the South China Sea. Lower and middle Miocene deposits are reported from India (Xu et al., 2015; Sarkar et al., 2024; Ghosh et al., 2017) and in the Neogene Mut basin in southern Turkey (Vescogni et al., 2014).

The best documented and most abundant late Miocene bioherms are limited to the early Messinian of the Mediterranean Basin, particularly in the Sorbas and Nijàr basins of southeastern Spain (Mankiewicz, 1988; Franseen and Mankiewicz, 1991; Martín and Braga, 1994; Braga et al., 1996; Braga and Martín, 1996; Martin et al., 1997; Reolid et al., 2014). Other scattered deposits are present in the Melilla Basin of Morocco (Cornée et al., 1996; Saint Martin and Cornée, 1996; Roger et al., 2000; Münch et al., 2001; Cunningham and Collins, 2002), the Bas-Chelif Basin of Algeria (Saint Martin et al., 1992; Cornée et al., 1996, 2004), in the Salento Peninsula in southeastern Italy (Vescogni, 2000; Bosellini et al., 2001, 2002), and in Crete Island (Brachert et al., 2007). The occurrence and distribution of *Halimeda* in the Pliocene and Pleistocene remains poorly understood due to incomplete documentation.

Considering that known Upper Miocene *Halimeda* bioherms are limited to the Mediterranean area, the main objective of this study is to gain insights into the controlling factors responsible for their development during this specific time interval. As a case of study, we examined two *Halimeda*-rich deposits, exposed along the upper slope of a Messinian Reef Complex in the Salento Peninsula (southeastern Italy) and previously interpreted as belonging to the Novaglie Formation slope system, with a depth of at least 30–50 m (Bosellini et al., 2002). We also here compared our results with coeval fossil and modern examples from various locations worldwide to assess differences and similarities in the morphology of these structures, as well as the external factors controlling bioherm development and extent.

2. Geological settings and stratigraphy

The Salento Peninsula constitutes the southernmost margin of the Apulia Carbonate Platform (ACP), one of the peri-Adriatic carbonate banks that developed during Mesozoic and Cenozoic times in the southern portion of the Tethyan Ocean (Bernoulli, 2001; Morsilli et al., 2017; Morsilli et al., 2021). The ACP extends from the Gargano Promontory to the Cape Leuca, in the Apulia region (Fig. 1). Starting from the late Cretaceous, the Salento Peninsula was characterized by shallow-water deposition, influenced by moderate sea level oscillations (Bosellini et al., 1999). The Paleogene and Neogene sediments were deposited in several graben structures related to the tensional tectonic regime that characterizes the Salento Peninsula (Martinis, 1962; Tozzi, 1993). Presently, along the eastern coast of the Salento Peninsula, from Capo d'Otranto to Santa Maria di Leuca (Fig. 1), there is a continuous exposure of Late Cretaceous to Quaternary successions mainly consisting of carbonate rocks including several reef tracts displaying a complex stratigraphic architecture. In fact, this carbonate stacking pattern occurs with lithostratigraphic units that are not simply stacked one above the other; rather, they appear reduced in size and very thin at the platform top, while relatively numerous and thick along the margin and slope. These units are grafted upon one another and separated by sharp unconformities (Bosellini et al., 1999) (Fig. 2).

In the Salento Peninsula, the upper Cretaceous succession consists of shallow-water facies, from the inner platform to the high energy margin (Fig. 2). The lithostratigraphic units, including the Melissano Limestone (early Campanian), the Santa Cesarea Limestone (mid-Campanian/lower Maastrichtian) and the Ciolo Limestone (upper Maastrichtian) were studied because of the exceptional occurrence of rudist association (Cestari and Sirna, 1987; Laviano, 1996; Bosellini et al., 1999).

These Cretaceous units are unconformably overlain by Eocene, Oligocene, Miocene, and Plio-Pleistocene carbonate strata (Fig. 2). The sequence begins with Torre Tiggiano Limestone (Lutetian/Bartonian), Torre Specchialaguardia Limestone (Priabonian) Castro Limestone (lower Chattian) and the Porto Badisco Calcarenites (upper Chattian) (Nardin and Rossi, 1966; Bosellini and Russo, 1992; Bosellini et al., 2001; Bossio et al., 1994; Parente, 1994; Bosellini, 2006; Pomar et al., 2014). In middle Miocene times, this area experienced a rapid tectonic subsidence related to the advance of the Apennine chain, resulting in the tectonic subsidence of the Salento Peninsula and consequent flooding, with the deposition of a thin, condensed layer known as Aturia Level along the margin (Serravalian/Tortonian) (Föllmi et al., 2015; Vescogni et al., 2018). During the lower Messinian, a well-developed coral reef system, the Novaglie Formation, and coeval back-reef deposits the Andrano Calcarenites were deposited (Bosellini et al., 1999; Bosellini et al., 2001, 2002; Vescogni et al., 2008). The top of the Novaglie Formation (NF3) is considered the Terminal Carbonate Complex (TTC) preceding the Messinian Salinity Crisis (Vescogni et al., 2022). The Novaglie Formation is unconformably overlain by the Leuca Breccia Formation and the Uggiano la Chiesa Formation (Piacentian/Gelasian). The deposition of the Salento Calcarenites marks the last sedimentary unit in the Salento Peninsula (Bosellini et al., 1999; Tropeano et al., 2022).

3. The Novaglie Formation

The early Messinian in the Salento Peninsula is represented by two heteropic stratigraphic units, the Andrano Calcarenites and the Novaglie Fm. The first is characterized by back-reef deposits that occupy the most internal areas of the carbonate platform, while the second one includes reefal limestone which occur in the present-day coastal area (Figs. 1 and 2). This unit is discontinuously exposed along the eastern coast of the Salento Peninsula from Tricase Porto to S.M. di Leuca for a total length of 17 km (Fig. 1) and was dated to the early Messinian (Bosellini et al., 1999; Bosellini et al., 2001) based on benthic foraminifera and ostracods associations. This unit shows a well-developed reef complex with monogeneric *Porites* exhibiting various morphologies (Fig. 3), and clinostratified breccia forming prograding slope and distal-slope deposits (Bosellini et al., 2001, 2002; Bosellini, 2006). This reef complex was generally characterized by heterogeneous reef-building biota such as *Porites* corals, scattered *Halimeda* bioherms, coralline algae, and

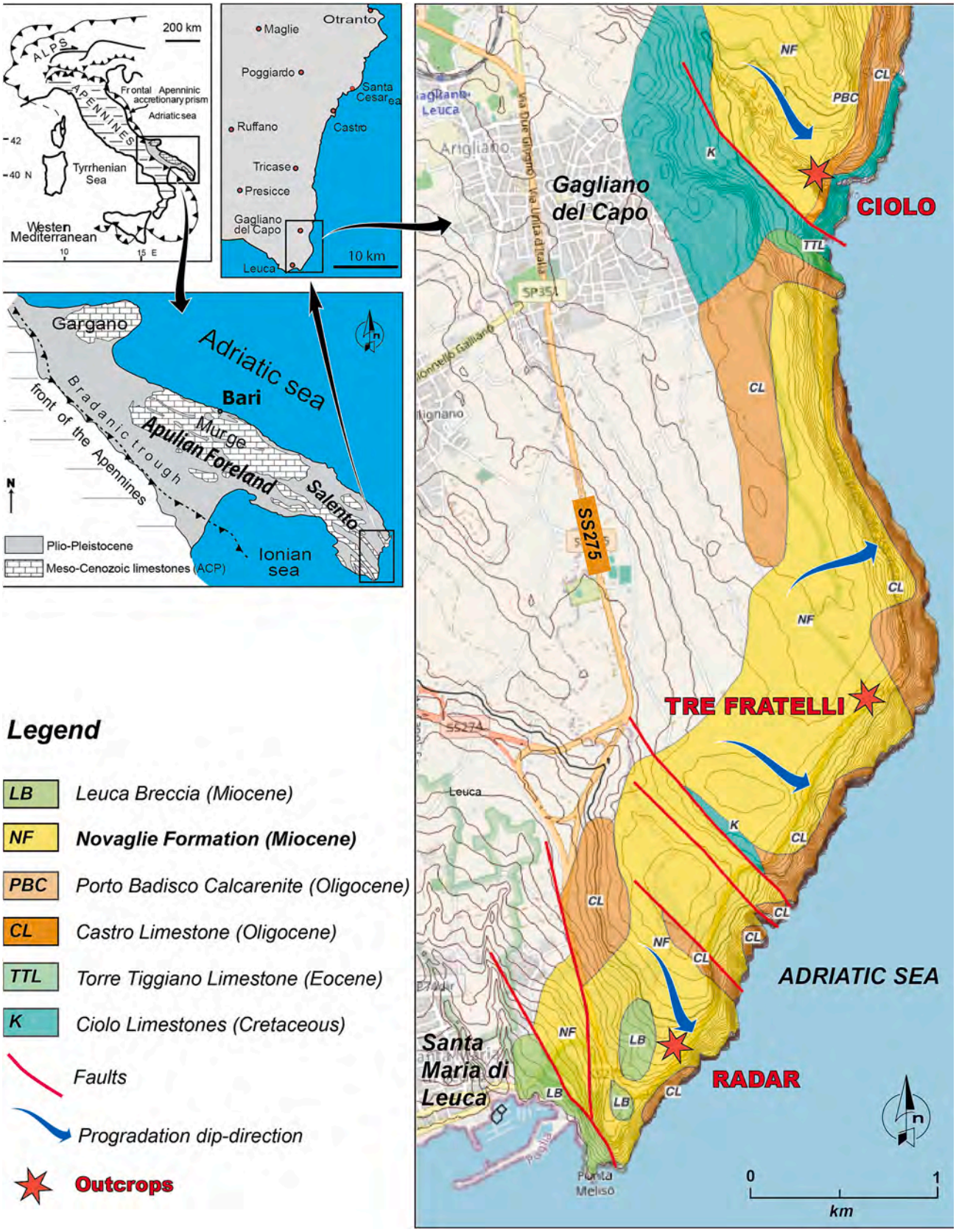

Fig. 1. Location map of the Salento Peninsula and of the study sites. A) structural and geological settings; B) map of the outcropping formations along the southeasternmost margin of the Salento Peninsula (modified after Bosellini et al., 1999).

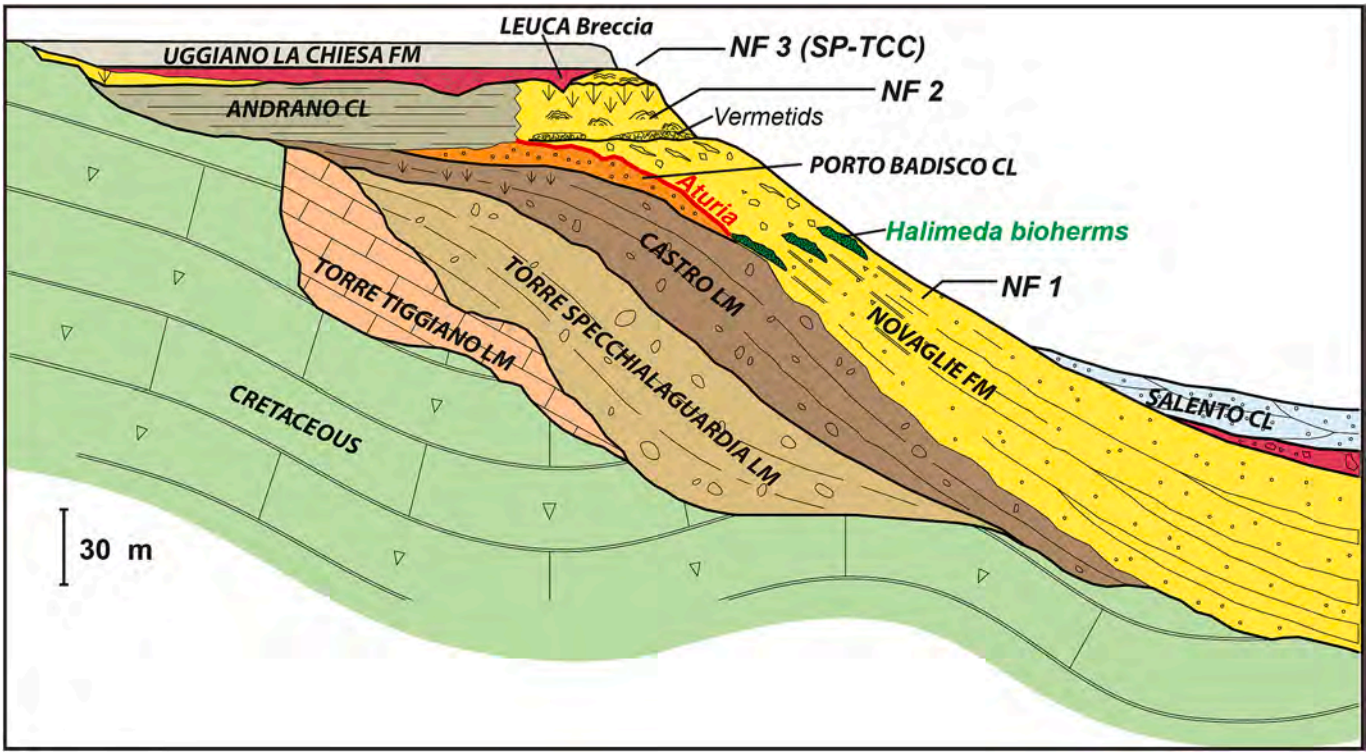

Fig. 2. Stratigraphic architecture of the southeastern Salento Peninsula: Upper Cretaceous substrate, Torre Tiggiano Limestone (Lutetian/Bartonian), Torre Specchialaguardia Limestone (Priabonian), Castro Limestone (middle-upper Chattian), Porto Badisco Calcarenite (uppermost Chattian), Aturia level (Serravallian/Tortonian), Andrano Calcarenites (lower Messinian), Novaglie Formation (lower Messinian), Leuca Breccia (upper Messinian), Uggiano la Chiesa Fm. (Piacenzian/Gelasian), Salento Calcarenites (lower Pleistocene) (modified after Bosellini et al., 1999 and Vescogni et al., 2022).

vermetid-microbial bioconstructions along with encrusting foraminifera, bryozoans and serpulids (Bosellini et al., 2002; Bosellini, 2006).

A review of the reef architecture was carried out by Vescogni et al. (2022). The reef complex consists of three main superimposed units each separated by erosional surfaces (Fig. 2). The first unit, NF1, is 120 m thick and shows a complete margin-to-slope reef tract with reef rubble, meters thick *Halimeda* bioherms and packstones, rhodolith floatstones-rudstones, and bioclastic calcarenites dated to the early Messinian (7.3–5.87 Ma). The overlying NF2 unit, 20 m thick, consists of *Porites* coral framework which thins out toward the proximal slope. The last unit, NF3, characterized by 10 m thick oolitic deposits associated with microbialites, colonies of *Porites*, and small vermetid and serpulid bioherms (Bosellini et al., 2001, 2002), upper Messinian in age (5.97–5.60 Ma), is interpreted as equivalent to the TCC (Terminal Carbonate Complex) related to the Messinian Salinity Crisis (MSC) (Bosellini et al., 2001; Vescogni et al., 2022). The TCC is capped by the Leuca Breccia Formation characterized by an up to 12 m thick breccia layer containing clasts derived from the underlying Novaglie Formation (Bosellini et al., 1999; Vescogni et al., 2022).

The age of the Novaglie Formation was established as early Messinian, coeval with the Andrano Calcarenite, based on the identification of the benthic foraminifera *Bulimina echinata*, which was found in both Formations. The presence of the characteristic taxa assemblage, including the ostracods *Pokornyella italica*, *Pokornyella devians, Aurila albicans, Aurutella saheliensis,* and *Aurilia stabilis*, further support an early Messinian age (Bosellini et al., 2001).

4. Materials and methods

We measured and analyzed in detail two stratigraphic sections exposed on a road cut along the coast between the localities of S.M. di Leuca and Ciolo (Fig. 1).

We characterized two *Halimeda* bioherms in two distinct stratigraphic sections. The "Tre Fratelli" section is 15 m thick, the "Radar" section, located 2 km to the south of the "Tre Fratelli", is 17 m thick. Both the bioherms studied were previously interpreted as belonging to the NF 1 slope system, with a depth of at least 30–50 m (Bosellini et al., 2002). To document the textural variations observed, the outcrop was subdivided into 10 sectors (A–L) according to the organization of the algal segments starting from the contact with the underlying vermetid accumulation.

Both sections were sampled at a scale ranging from decimeters to meters at each change in facies or texture. However, in facies characterized by a high density *Halimeda*, samples were collected every ten or twenty centimeters (Fig. 5A). This higher sampling density allowed for more accurate taphonomic observations across the *Halimeda* accumulations. From both sections, a total of 54 rock samples were collected. Specifically, 35 samples were collected from the "Tre Fratelli" section, with 22 of those taken from the interval where the *Halimeda* bioherm is present. Meanwhile, 19 samples were collected from the "Radar" section, with 12 of those from the interval containing *Halimeda* facies. The samples were then reduced into billets using a REMET TR 80 petrographic cutting saw for the preparation of an equal number of standard-

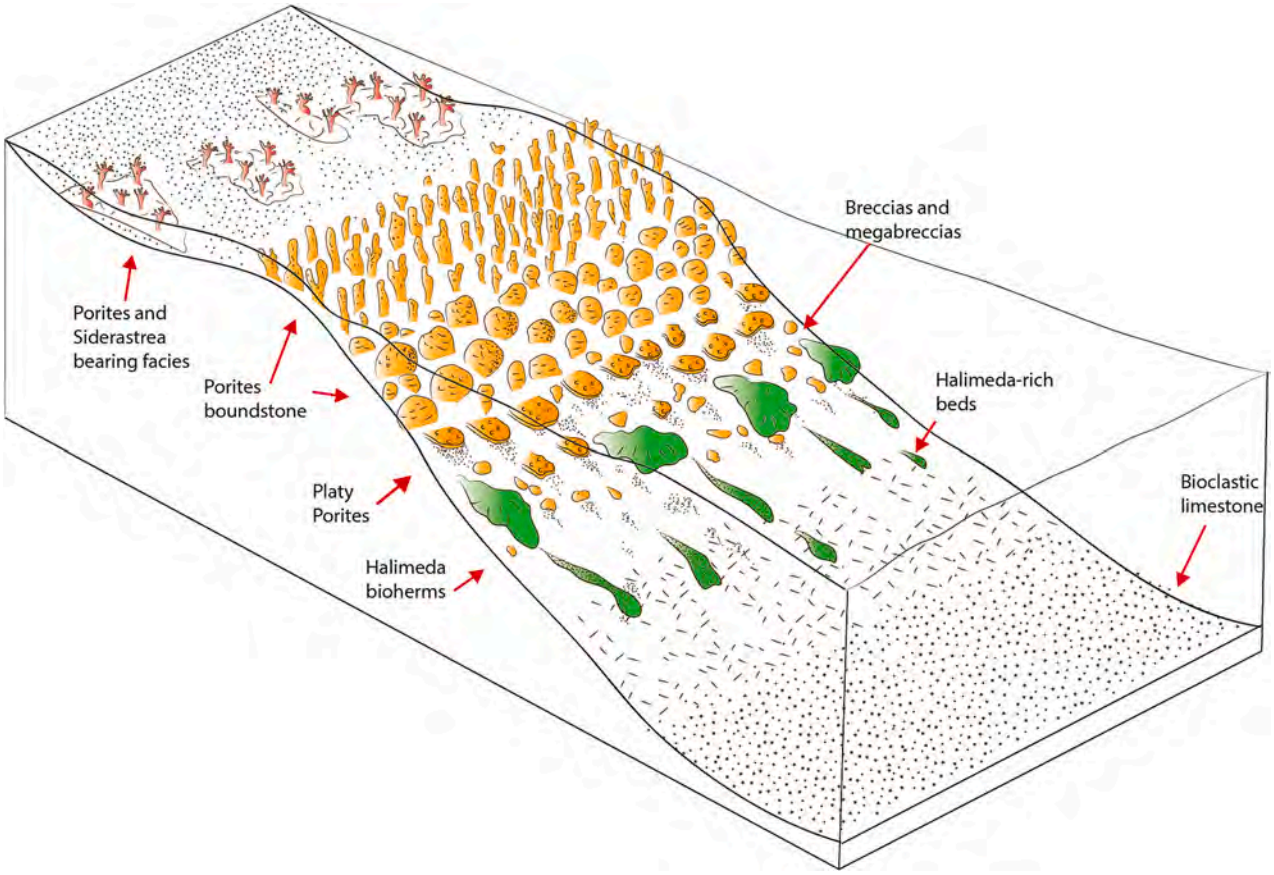

Fig. 3. Depositional model of NF1 showing position of *Halimeda* bioherms and *Halimeda* rich-beds on the proximal-to-mid slope and zonation of Porites coral with different morphologies and main facies types (slightly modified after Bosellini and Russo, 1992).

Fig. 4. Outcrop aerial view reconstruction through Agisoft metashape software of the "Tre Fratelli" bioherm with a strategic strike cut between two roads, allowing for geometric relationships and detailed description of the internal organization of the *Halimeda* bioherm.

Fig. 5. Reconstruction through Agisoft Metashape software of the two outcrops, highlighting the facies and the location of the samples collected: the dark green areas highlight the occurrence of *Halimeda* thalli in growth position (HB facies) while in light green, areas with rudstones-floatstones textures (HRF facies). A) Draw-line of the outcrop "Tre Fratelli" showing the internal organization of the deposit. In pink, the vermetids bioherm. Below: two enlargements of two sectors of the outcrop (B – G) with the algal segments orientation. B) In dark-green, levels where the algal thalli are identified in growth position in the "Radar" outcrop. See Fig. 6 for facies color legend.

sized thin section (30 × 45 mm). The thin sections were then examined under a transmitted light microscope, and the observations were integrated with field descriptions for to determine the lithofacies. This analysis facilitated the identification of microfacies, with the percentage of bioclasts relative to the matrix estimated visually. Description of textures were based on Dunham (1962), Embry and Klovan (1971) and Insalaco (1998) classification diagrams.

Photogrammetric surveys were collected along the outcrops using a DJI Mavic Pro UAV fitted with a high-resolution camera capable of capturing images with resolutions up to 12 megapixels. The images were processed using Agisoft Metashape software to generate 3D point clouds, orthomosaics, and digital outcrop models (DOMs).

5. Results

5.1. The "Tre Fratelli" stratigraphic section

The stratigraphic section "Tre Fratelli" (Fig. 6), located in the proximal-to-mid slope of NF 1 (Bosellini et al., 2002), begins at the ground level, with a thick interval of vermetids reaching a thickness of about 2 m. This accumulation is characterized by boundstone textures, featuring area of significant primary porosity. In some locations, this porosity is filled with fine sediments, while in other, large botryoidal aragonitic cements have precipitated (Fig. 9A-B-C1-C2-D). Additionally, extensive areas contain reddish geopetal structures, with cavity walls lined with thin isopachous calcite cements (Brachert et al., 2007).

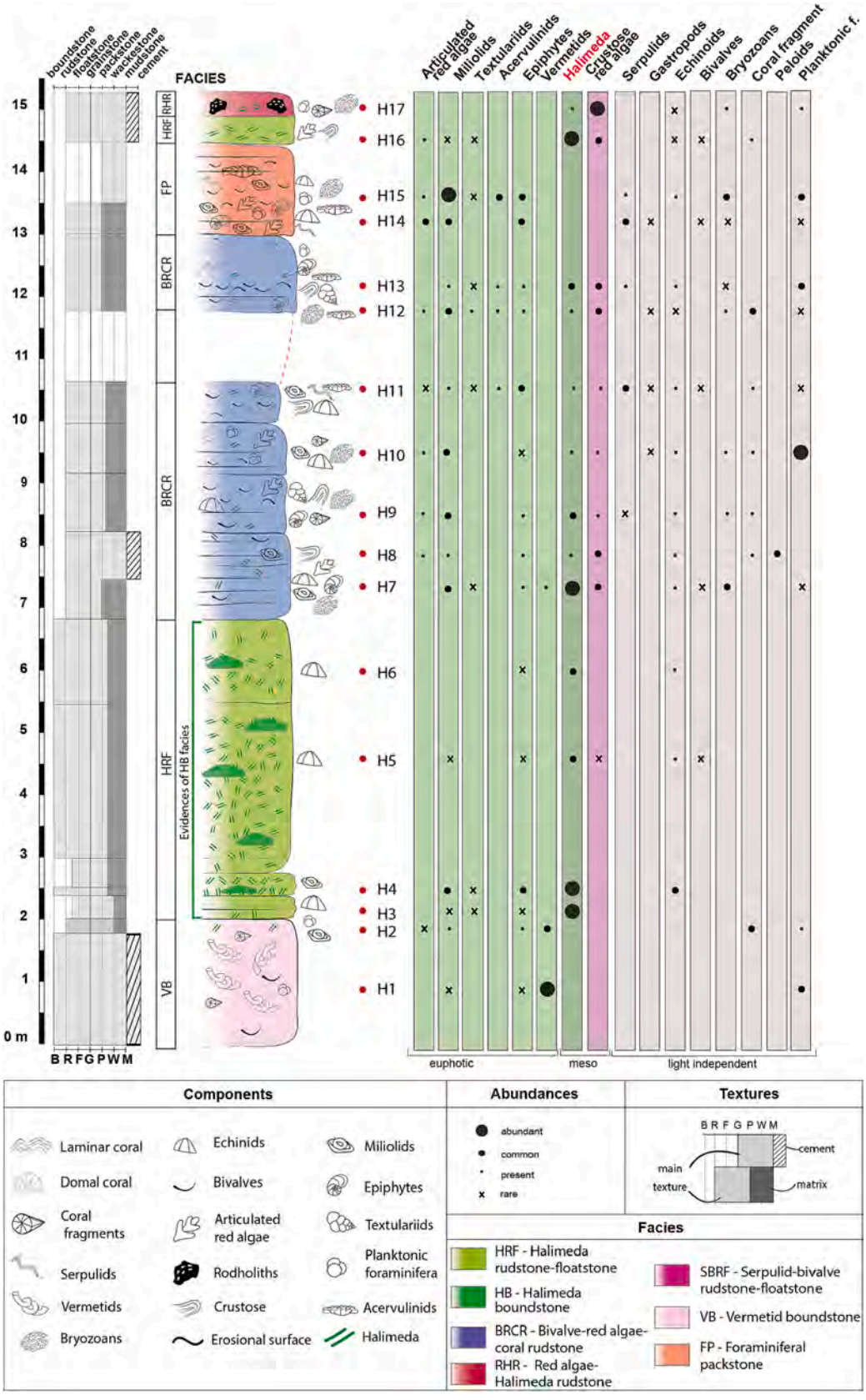

Fig. 6. Stratigraphic log of the "Tre Fratelli" section featuring sample locations, textures, facies, and abundances of the respective components. Within the HRF facies (highlighted in bright green), the vertical orientation of *Halimeda* segments indicates autochthonous accumulation, represented by HB facies in dark green (See Table 1 for facies description).

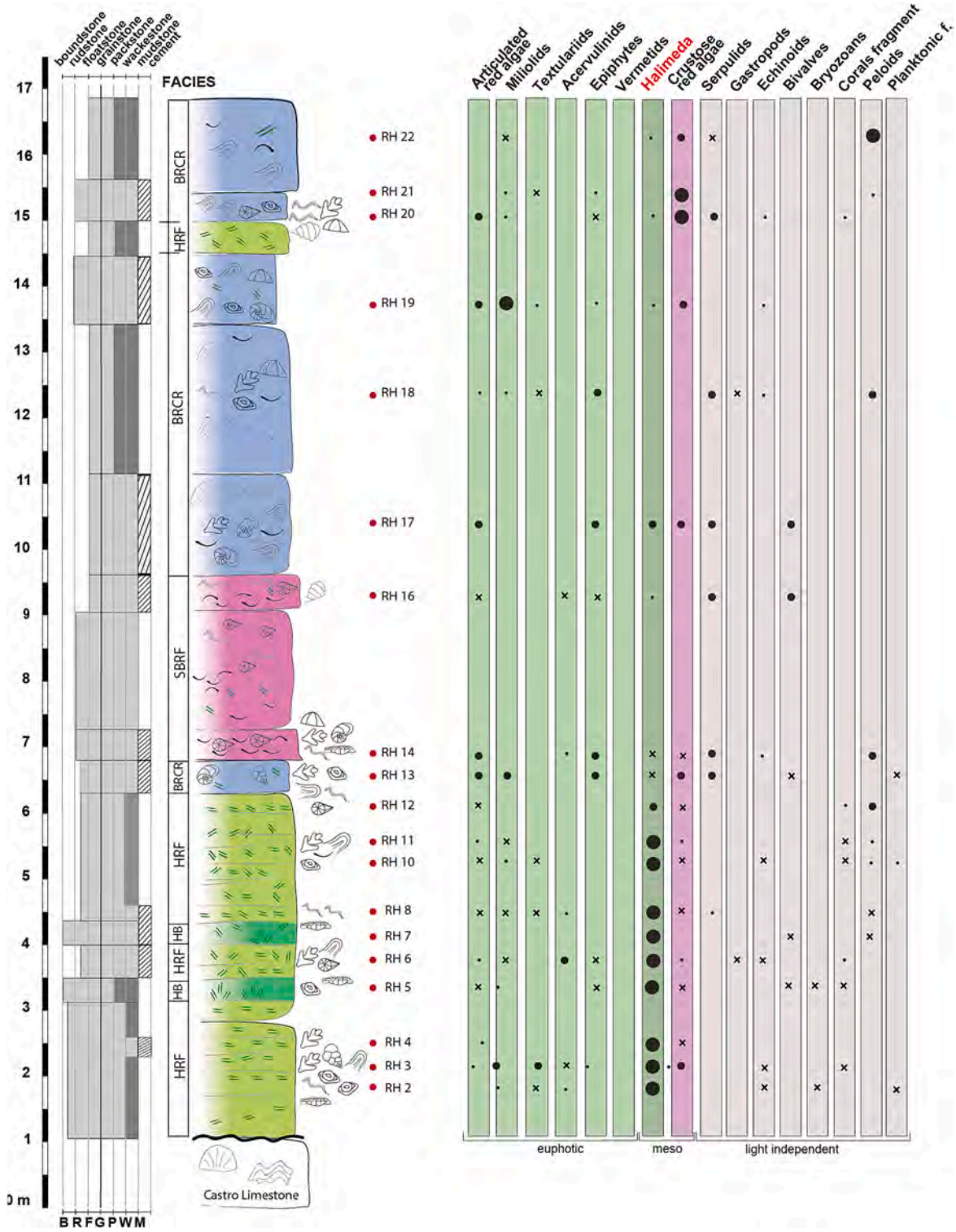

Fig. 7. "Radar" Stratigraphic log featuring sample locations, textures, facies, and abundances of the respective components on the base of the photic zone. The dark green areas identified by the HB sub-facies, where the *Halimeda* segments are vertically oriented, indicate autochthonous sedimentation, while the right green areas identified by the HRF facies, where the algal segments are disorganized or imbricated, reflect areas of allochthonous sedimentation (See Table 1 for facies description and Fig. 6 for symbols legend).

Table 1
Recognized facies of the Tre Fratelli and Radar sections with the relative abundance of components. Studied samples and fossil content are expressed as: a-abundant, c-common, p-present, r-rare.

Facies	Matrix	Cement	Skeletal components	Remarks
HRF - *Halimeda* rudstone - floatstone	Packstone to poorly sorted wackestone	Isopachous calcite	*Halimeda* (a); articulated and crustose red algae (c), miliolids (c), acervulinids (c), planktonic foraminifera (p)	Peloidal micrite
HB - Halimeda boundstone	Packstone to poorly sorted wackestone	Fibrous isopachous calcite, thin micritic calcite crust, fibrous aragonite, isopachous calcite	*Halimeda* (a), pectinids (r), planktonic foraminifera (r)	Very well preserved *Halimeda* segments in growth position with high intergranular porosity
RHR - Red algae - *Halimeda* rudstone	Fine wackestone	Fibrous and isopachous calcite layers	Crustose red algae (a); *Halimeda*, bryozoans, planktonic foraminifera (p)	Red algae encrustations
VB - Vermetid boundstone	Wackestone to packstone; mudstone pockets	Botryoidal aragonite; isopachous calcite	Vermetids in growth position (a); coral sticks, planktonic foraminifera (c); epiphytes, miliolids (r)	Geopetal infills; high intergranular porosity
BRCR - Bivalve - red algae - coral rudstone	Packstone to wackestone		Bivalves, crustose red algae (a); laminar and domal corals in growth position, Porites fragments, Halimeda, articulated red algae (c); miliolids, epiphytes, acervulinids, planktonic foraminifera (p); fragments of echinoids and bryozoans (r)	
SBRF - Serpulid - bivalve rudstone - floatstone	Fine reddish wackestone	Isopachous calcite	Serpulids, bivalves (a); coral sticks, gastropods, *Halimeda*, elphidium, acervulinids (c)	
FP - Foraminiferal packstone			Miliolids, textulariids, epiphytes (a); bivalves, fragmented articulated red algae, serpulids, bryozoans, echinoids (c-p); planktonic foraminifera (c)	

The vermetid accumulation is overlain with a gradational contact, by a 4.85 m thick interval rich deposit rich in *Halimeda* plates, characterized by a high concentration of densely packed algal segments. The road cut, dissected by two roads that intersect about 30° and featuring a fresh surface, has enabled detailed observations of lateral variations in facies within this deposit (Fig. 4).

This bioherm is organized in centimeter-scale zones or convex lenses consisting of vertically arranged *Halimeda* segments with a packstone to wackestone matrix. Locally, where the matrix is absent, these small boundstone lenses are characterized by high depositional porosity, filled with abundant early-diagenetic cement. The algal segments encrusted by the cement are well-preserved. The *Halimeda* boundstone laterally transition to rudstone to floatstone textures, identified by a subtle stratification associated with the chaotic or imbricated arrangement of the algal segments. *Halimeda* segments is the predominant component, accounting for almost 80–90 % of the bioclasts, followed by *other skeletal components such as small benthic epiphytic foraminifera (miliolids and textulariids), fragments of Porites, echinoids, bryozoans, and non-articulated red algae.*

An abrupt change in components marks the top of the *Halimeda* accumulation, recorded by a sharp decrease in the abundance of the algal segments and the appearance of bivalve rudstone containing a few serpulid fragments. Additional fauna includes crustose and articulate red-algae, *Porites* coral fragments, and epiphytic benthic foraminifera (miliolids and textulariids). This interval reaches a total thickness of about 4.65 m being interrupted at the top by a meter of soil cover. Poorly stratified layers of foraminiferal packstone, rich in shallow-water benthic foraminifera, extend for 1.5 m, with a reappearance of the *Halimeda* rudstone-floatstone characterized by a 0.5 cm thick layer. The top of the section consists of a thin layer (0.5 cm) of rudstone-floatstone containing crustose red algae interspersed with few scattered *Halimeda* segments.

5.2. The "Radar" stratigraphic section

The 'Radar' stratigraphic section (Fig. 7) starts at the top of the Oligocene Castro Limestone. The base of the section consists of a diffuse contact and begins with layers of *Halimeda* rudstone-floatstone, which are 0,5 m thick, reaching a total thickness of 5.25 m, within which there are centimeter-scale boundstone lenses containing very well-preserved algal segments and filled with abundant early-diagenetic cements. The edges of these lenses are characterized by rudstone-floatstone textures, with segments chaotically dispersed or imbricated.

A sharp upper contact marks the transition to a 0.5 m layer of bivalve-rich rudstone with a wackestone matrix, containing a few serpulid fragments, crustose and articulated red algae, fragments of *Porites* corals, and epiphytic benthic foraminifera such as miliolids and textulariids. This layer is capped by a massive layer that is 2.85 m thick, mainly characterized by an abundance of densely-packed serpulids, with scattered bivalve shells. The top of the section consists of 6.7 m of bivalve-rich rudstone, interrupted by a 0.5 m layer of *Halimeda* rudstone-floatstone (Fig. 7).

5.3. Facies description

Field and thin section analysis allowed the identification of six facies (Table 1) with textures spanning from rudstone-floatstone to packstone in which the biota is mainly represented by *Halimeda*, other encrusting organisms like vermetids, serpulids and red algae, including shallow-water benthic foraminifera, bivalve shells and corals sticks.

5.3.1. HRF - Halimeda rudstone-floatstone

The HRF facies is the most abundant within the two measured sections. It is predominantly characterized by chaotically to imbricated jumbled *Halimeda* segments within a packstone to poorly sorted wackestone matrix, where a relatively small amount of other skeletal grains can be observed, such as articulated and crustose red algae, echinoids, bryozoans, pectinids, and miliolids and planorbulinids (Fig. 8E). A peloidal micrite, probably of microbial origin is visible in thin section (Fig. 8E–F).

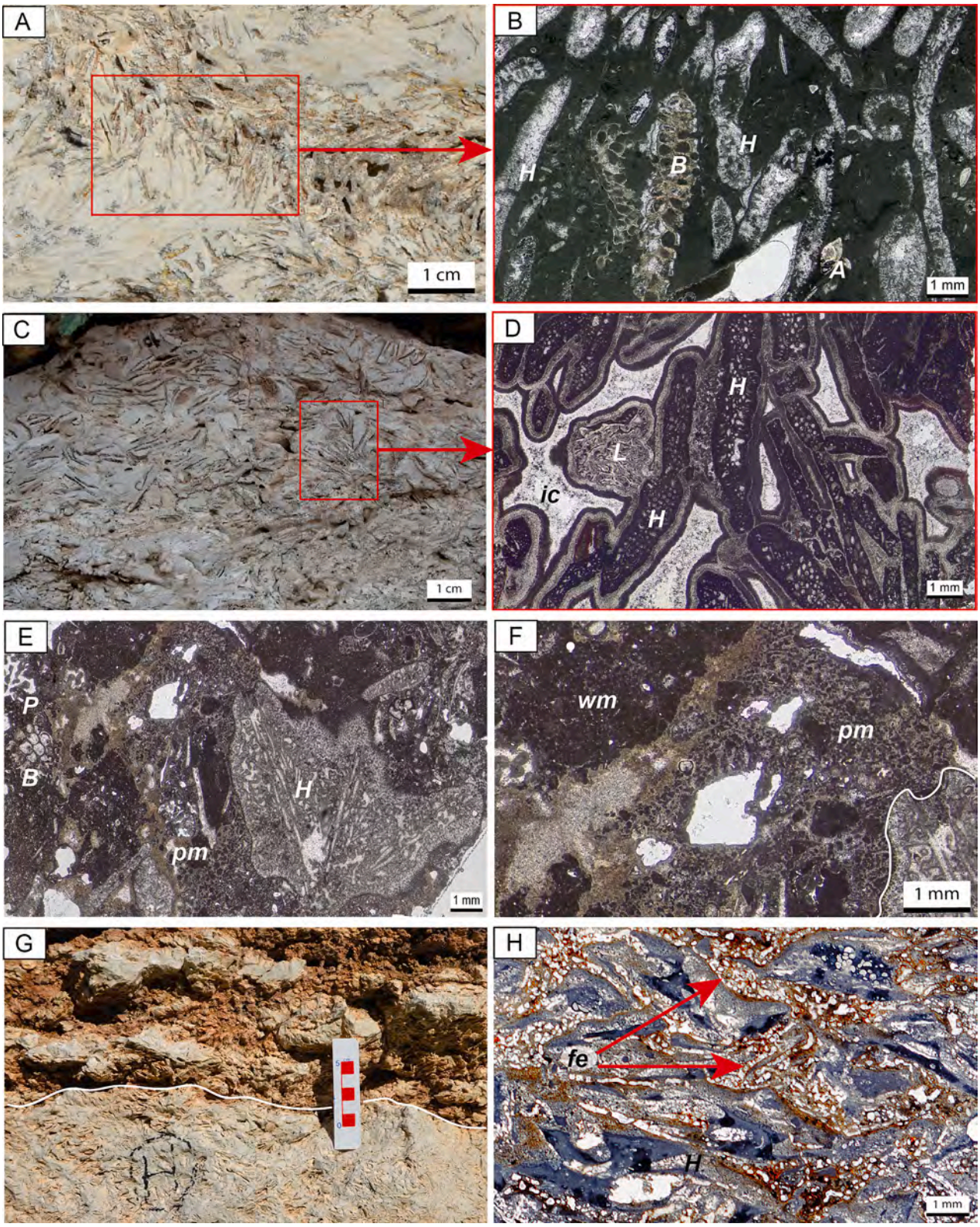

Fig. 8. Thin sections of the *Halimeda* facies A–B) HB facies: the vertically oriented algal segments (H) with a fine wackestone to packstone matrix indicate in-situ production of *Halimeda* (red squares). Other components include bryozoan fragments (B) and shallow-water benthic foraminifera like amphisteginids (A). C–D) HB facies: here the vertically oriented very well-preserved *Halimeda* segments (H) occur rimmed by up to four different generation of pre-diagenetic marine cements (red square), including a last stage of isopachous calcite infills. Other components are encrusting foraminifera such as *Laduronia* sp. (L). E) HRF facies: *Halimeda* segments (H) with a packstone to wackestone matrix encrusted by a peloidal micrite crust (pm). Other common components are fragments of bryozoans (B) and Porites corals (P). F) HRF facies: close-up on the peloidal micrite encrusting a well-preserved *Halimeda* segment (white line). G) HRF facies: a close-up detail of the terminal (flank) portion of the bioherm in the "Tre Fratelli" section where the deposit appears less massive and more stratified due to the horizontally to imbricated arrangement of *Halimeda* segments. H) HRF facies: *Halimeda* segments in a fine wackestone matrix affected by abundant foraminiferal encrustations (fe) (red arrows).

5.3.2. HB - Halimeda boundstone

This facies is represented by convex lenses that thin out and is characterized by vertically oriented *Halimeda* segments (Fig. 5A, 8A, C). The frame cavities are partially filled with wackestone matrix (Fig. 8A–B), while the remaining cavities are filled with two different generations of *syn*-depositional cement characterized by an early layer of fibrous isopachous aragonite, followed by an isopachous calcite crust with bladed crystals (Fig. 8D). The preservation quality of the *Halimeda* segments varies significantly, ranging from very high to low. High-quality preservation ensures that the internal structures of the segments remain well-defined, while low-quality preservation results in an indistinct or entirely dissolved structure, leaving molds. Occasionally, these molds are filled with sparry calcite.

5.3.3. VB - vermetids boundstone

This facies occurs at the base of the "Tre Fratelli" section where it

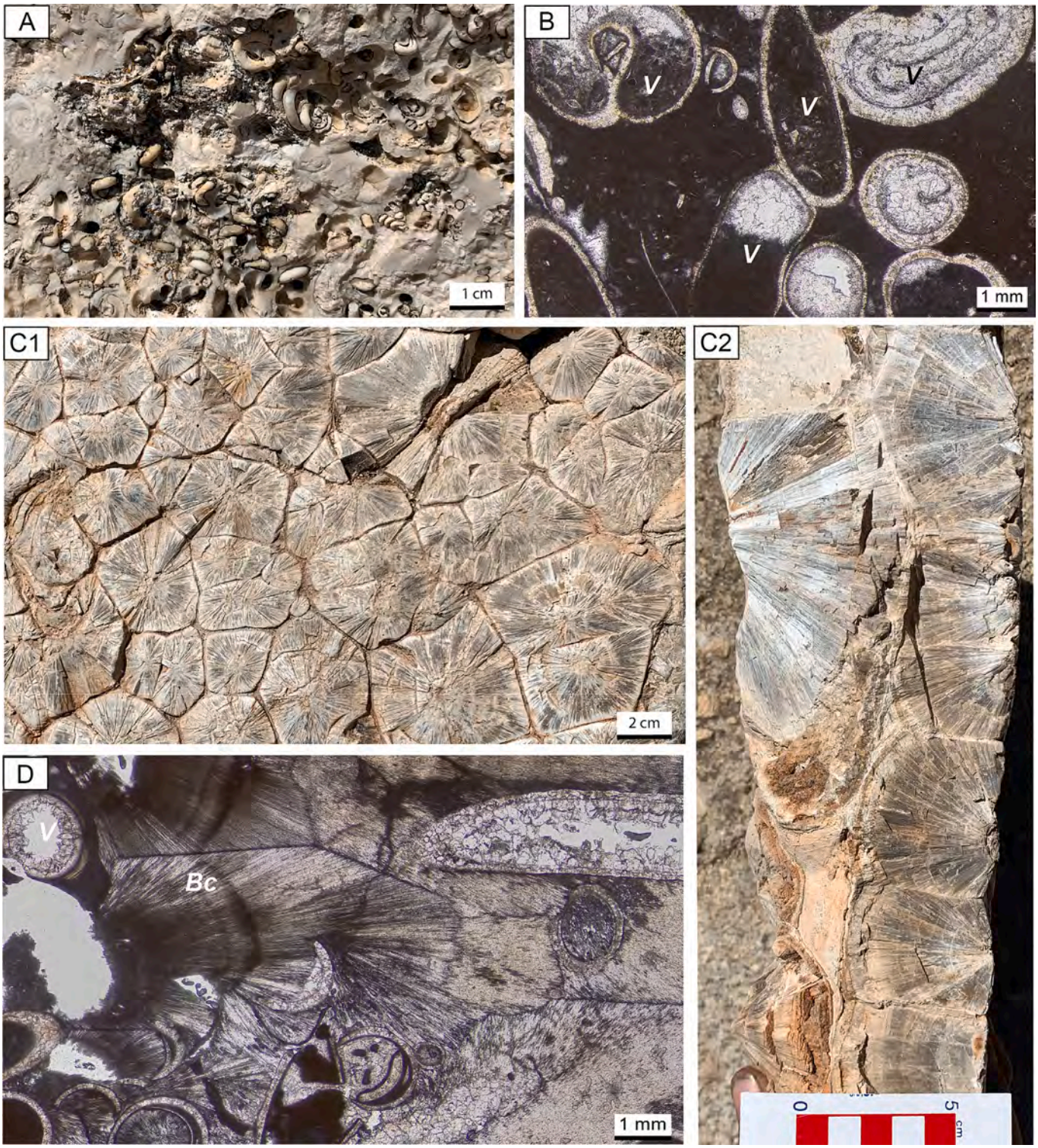

Fig. 9. A) VB facies: outcrop close-up of arranged vermetid tubes in a with wackestone matrix. B) VB facies: thin sections of arranged vermetid tubes (V) in a wackestone to mudstone matrix with some geopetal infills. C1 and C2) VB facies: the large quantity of aragonitic botryoidal marine cements that fill the porosity up to a maximum of 60 %. D) VB facies: detail of the aragonitic botryoidal cements (Bc) and vermetid tubes (V).

reaches 2 m in thickness (Fig. 9A). This facies is characterized by recrystallized vermetids and a few *Porites* fragments and contains cavities filled with wackestone-packstone matrix. Other common components include bivalves, bryozoans, echinoids, along with miliolids and textulariids, and few planktonic foraminifera. Notably, some vermetids tubes exhibit geopetal infills characterized by vadose silt and drusy calcite (Fig. 9B). Locally, massive early botryoidal aragonite cement fills 40–60 % of the remaining cavities (Fig. 9C1-C2-D).

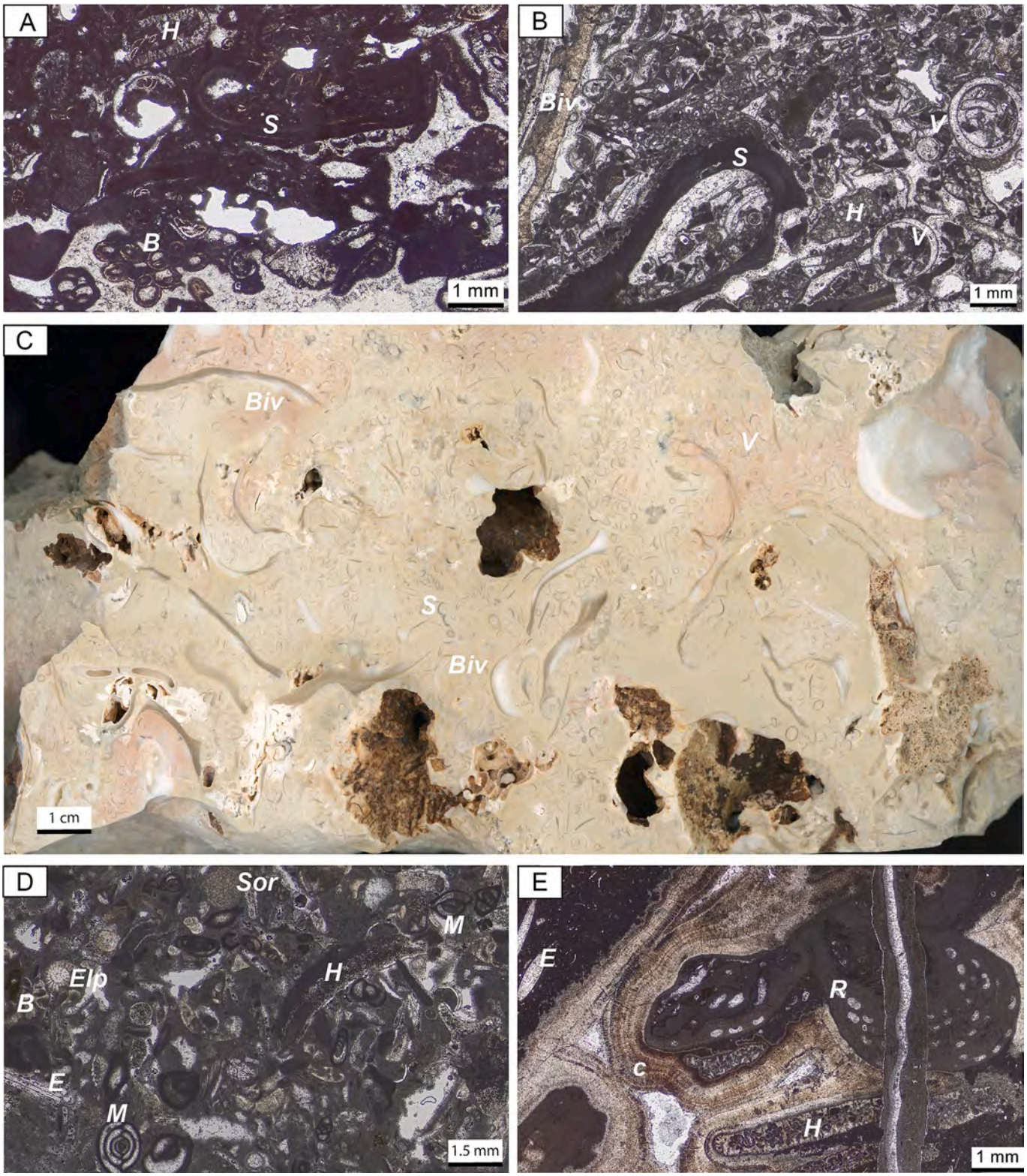

Fig. 10. A) BRCR facies: thin section with serpulids (S), bryozoans (B) and *Halimeda* segments (H). B) SBRF facies serpulid fragments (S) along with bivalves (Biv), vermetids and *Halimeda* segments (H) within a peloidal matrix and isopachous cements. C) SBRF facies: polished slab with serpulids (S), vermetids (V) and bivalve fragments (Biv). D) FP facies: arrangement of shallow-water benthic foraminifera like miliolids (M), soritids (Sor), textulariids (T), amphisteginids (A) along with few echinid spines (E), bryozoans (B), and *Halimeda* segments (H). E) RHR facies: crustose red algae (R) and well-preserved *Halimeda* segments (H) held together by various generations of cements (c)filling the high intergranular porosity, along with a fine wackestone matrix rich in planktonic foraminifera and echinid spines (E).

5.3.4. BRCR - bivalve-red algae-coral rudstone

This facies comprises beds ranging from decimeters to meters in thickness and is characterized by the prevalence of large bivalve molds. Additional biota includes, domal to platy *Porites* coral fragments and crustose and articulated red algae (Fig. 10A). Common components include *Halimeda* segments, miliolids, epiphytes such as *Elphidium and Amphistegina*, and planktonic foraminifera. Less abundant occurrences are echinoids, serpulids and bryozoan fragments (Fig. 10A). Locally, cavities are filled with a packstone-wackestone matrix, while in other instances, they are filled with sparry calcite (Fig. 10A).

5.3.5. SBRF - serpulid-bivalve rudstone-floatstone

This facies is exclusively present in the "Radar" section, where it occurs as an interval 2.8 m thick. It is characterized by centimeter-thick layers of serpulid rudstone containing abundant isopachous calcite, interbedded with serpulid floatstone with a fine, reddish wackestone matrix. Common components include bivalves, gastropods, *Porites* coral sticks, articulated red algae, *Halimeda* segments (Fig. 10C), and benthic foraminifera such as acervulinids and epiphytes (*Elphidium*) (Fig. 10B).

5.3.6. FP - foraminiferal packstone

This grain-supported facies is exclusively present in the upper part of the "Tre Fratelli" section, with a total thickness of 1.5 m. Its identification is based on the abundance of small shallow-water benthic foraminifera, predominantly miliolids and epiphytes (e.g. *Amphistegina* and *Elphidium*) and planktonic foraminifera (e.g., *Globigerinoides*, *Globigerina*). In smaller quantities there are molds of large bivalves, fragments of bryozoans, articulate red-algae, serpulids, and echinoids (Fig. 10D).

5.3.7. RHR - red algae - Halimeda rudstone

The RHR facies consists of crustose red algae (*Mesophyllum*) rudstone, containing well-preserved *Halimeda* segments. Additional biota includes planktonic foraminifera, a few benthic foraminifera, including miliolids and textulariids, and rare bryozoans and acervulinids (Fig. 10E). Red algae and acervulinids commonly encrust other skeletal fragments. This facies exhibits a high primary intergranular porosity partially filled with fibrous and isopachous cement (Fig. 10E).

6. Interpretation and discussion

The *Halimeda* bioherm of the "Tre Fratelli" section was analyzed in detail thanks to the favorable outcrop conditions that permits a partial 3D view (Fig. 5A). In order to provide a detailed analysis, the bioherm was divided into approximately 1-meter sectors (A–L). Following a thorough taphonomic analysis, it was found that the first seven sectors of the outcrop (A–G) are more massive. These sectors are primarily characterized by rudstone-floatstone textures (HRF facies) with poorly preserved algal segments arranged chaotically or imbricated within a wackestone matrix (Fig. 8). Within this interval, boundstone lenses can be identified (dark green spots in Fig. 5A). The space between the algal segments is either filled with matrix (Fig. 8B) or, at times, with cement (Fig. 8D). These cements surrounding the segments seems to favor the preservation of their original orientation and their internal structure (Fig. 8D). Instead, where the segments are surrounded by wackestone, they have been partially or completely altered. The bioherm laterally gradually thins out and becomes stratified in the terminal part, as observed in the last sectors (H–L) (Fig. 5). The stratification is due to presence of a succession of thin layers of floatstone containing largely dissolved imbricated segments, although zones characterized by boundstone textures persist. These stratified area (H–L interval) dominated by HRF facies are interpreted as the flank deposits of the boundstone accumulations (A–G interval) (Fig. 5A).

The "Tre Fratelli" bioherm exposure allows observing a variation between the more massive core and the flank, characterized by a reduced thickness and crude bedding. The internal architecture and facies distributions are consistent with a recent study by Reolid et al. (2024), that describe the internal organization of a modern mesophotic *Halimeda* mound in Tregrosse bank (Great Barrier Reef). On the basis of preserved depositional geometries of the Novaglie Formation (Bosellini et al., 1999), the *Halimeda* bioherms occur as part of a complex of small bioherms located in the mid-to-proximal slope of the Novaglie Formation reef (Fig. 11B–C).

6.1. Halimeda bioherms in the Messinian reefs of the Mediterranean area

While there are several documented occurrences of *Halimeda* in the Mediterranean during the Messinian, evidence of in-situ accumulations forming bioherms is scarce (Esteban, 1979; Brachert et al., 2007). Known examples in the literature are limited to southeast Spain, southeast Italy, and Crete where they typically develop along the reef slope area or as isolated mounds on ramp systems (Braga et al., 1996; Martin et al., 1997; Vescogni, 2000; Bosellini et al., 2002; Brachert et al., 2007).

Halimeda deposits in Crete have been interpreted by the authors as small, isolated in-situ accumulations (1.8 m wide and 0.6 m thick), associated with resedimented breccia, on the mid-to-proximal ramp (Brachert et al., 2007). These deposits share similar facies with the ones described in this paper, including significant early cementation. Nonetheless, resedimented *Halimeda*-rich beds are also abundant on Crete, indicating extensive *Halimeda* meadows development compared to what is found in the literature (Passaseo and Morsilli, 2024).

In the Sorbas and Nìjar basins of southeast Spain, extensive *Halimeda* deposits have been thoroughly documented from Tortonian and Messinian successions (Braga et al., 1996; Braga and Martín, 1996; Martin et al., 1997). According to Braga et al. (1996), the *Halimeda* bioherms of the Sorbas basin reach up to 400 m in length and 40 m in thickness and occur on a mid-to-proximal ramp with a gentle slope of about 5 degrees (Martin et al., 1997). The Salento deposits are smaller (~5 m in thickness) and located on a mid-to-proximal slope with a dip-angle between 15 and 30 degrees (Bosellini et al., 2002). Although, the different size and depositional setting, all these bioherms exhibit similar facies distribution and internal architecture, including the occurrence of *syn*-depositional marine cementation. However, the bioherms of Salento display more complex cementation with different types of cements, whereas the bioherms in Spain, are characterized by simpler, micritic and peloidal microbial crusts.

The differences in size and morphology of the bioherms may be attributed to the inclination of the slope, which directly affects the development and stabilization of the bioherms, or even to different nutrient availabilities. The high angle slope (up to 30°) was controlled from the morphology of the deep basin located in front of the Salento Peninsula, corresponding to the actual Otranto Strait (Bosellini et al., 1999). This is consistent with the fact that the large Holocene bioherms of the GBR (McNeil et al., 2016, 2021a,b, 2022; Reolid et al., 2024) develop on broad, sub-horizontal shelf.

In another area of the Sorbas Basin, a well-preserved fringing reef system near the locality of Cariatiz, features resedimented *Halimeda* deposit along the mid-to-proximal slope (Braga and Martín, 1996).

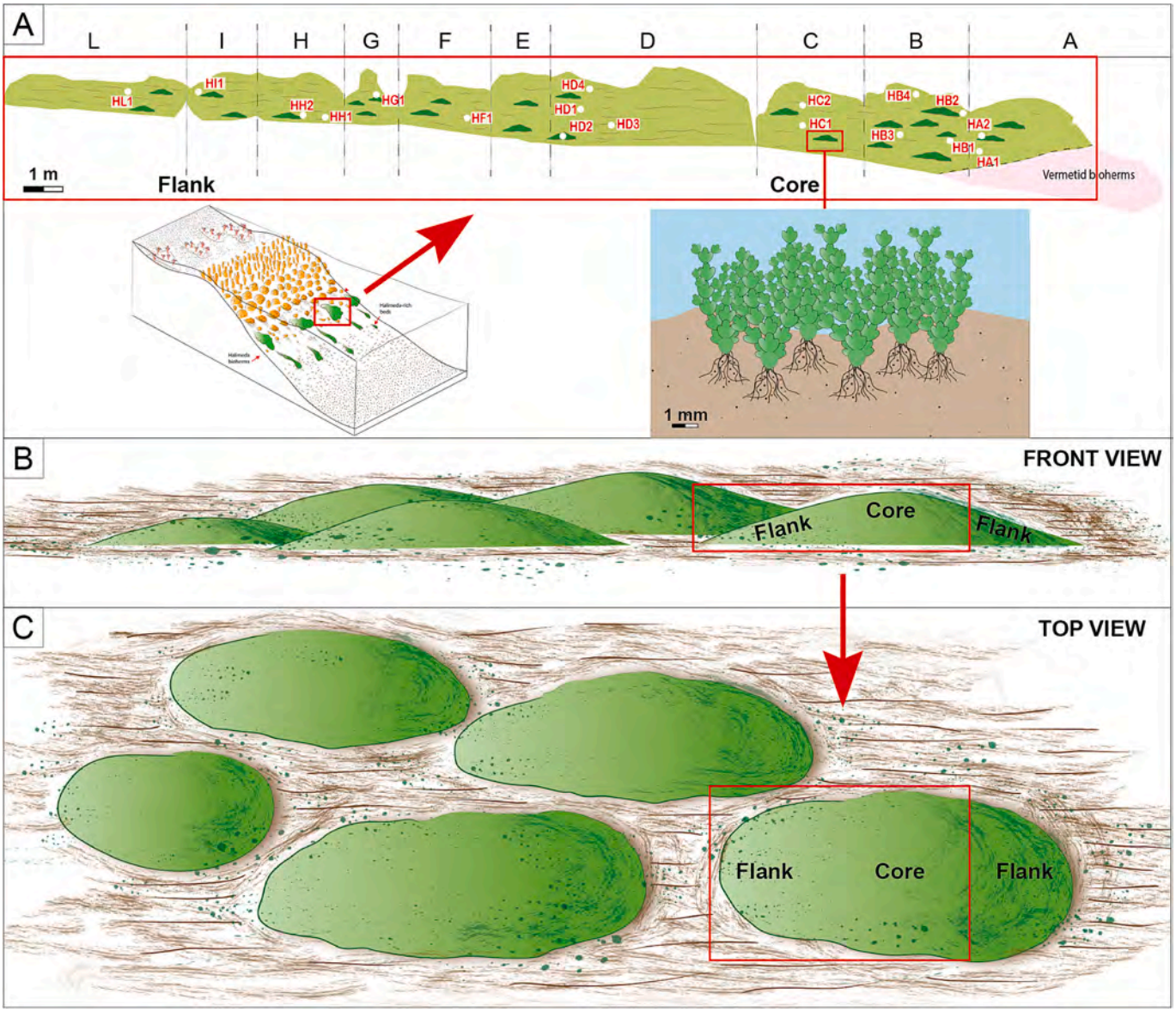

Fig. 11. Sketch of the depositional model and internal organization of the "Tre Fratelli" *Halimeda* bioherm subdivided in sectors (A–L) in scale located in the mid-to-proximal slope of the Novaglie Formation. A) Distribution of the facies HB (dark green) and HRF (bright green) within the outcrop. Algal thalli orientation in the HB facies. B) Inferred depositional model of the small *Halimeda* bioherm complex (not in scale). C) Top view. The red squares represent the outcropping zones of the bioherm in the Tre Fratelli outcrop.

Although these deposits are resedimented, they occur along the same slope position of the small bioherms of the Salento Peninsula.

6.1.1. Early diagenetic cementation

The succession of two early-marine cements surrounding the *Halimeda* segments in the HB facies (Fig. 8 D) and large botryoidal cements in the VB facies (Fig. 9 C1-C2-D), were observed only in the "Tre Fratelli" section. In the HB facies, it was observed that when cement occurs surrounding the algal segments, they are well-preserved. Conversely, when cement is absent and inly mud is present, the *Halimeda* segments are partially or totally dissolved. We infer that aragonitic cement acts as an impermeable film that prevents dissolution. This is because aragonitic cement exhibits greater resistance to dissolution than the algal segments, a resistance attributed its dense crystal fabric (Brachert et al., 2007). In addition, this early cementation preserves the vertical orientation of the segments suggesting an in situ accumulation. This accretion, combined with syn-sedimentary cementation, facilitated the development, accumulation, and stabilization of *Halimeda* bioherms on the steep slopes of the Novaglie Formation, as already documented in the bioherms from the Sorbas basin of Spain (Braga et al., 1996; Martin et al., 1997).

Early cementation in *Halimeda* bioherms has been documented not only from all three Messinian occurrences in the Mediterranean but also in *Halimeda* facies from offshore deposits of North Palawan – Philippines (Fournier et al., 2024). The specific nature of these cements and their occurrence in these facies remains poorly understood. During the early Messinian, the Mediterranean region began experiencing the initial effects of the salinity crisis (MSC), leading to the effective closure of major exchange routes with the Atlantic Ocean. The presence of marine syn-depositional cements within these facies suggests that specific geochemical conditions, possibly linked to the restricted water exchange during the onset of the (MSC), were critical in their formation. This restricted water exchange, combined with hypersaline bottom waters, and limited nutrient cycling, significantly affected marine biota, including *Halimeda* bioherms and coral reefs (Bosellini et al., 2002; Vertino et al., 2014; Moissette et al., 2018; Vasiliev et al., 2019; Mann

et al., 2022;Vescogni et al., 2022; Agiadi et al., 2024a,b). The $\delta^{18}O$ compositions of marine cements analyzed in the bioherms of Crete and Salento suggest that sea surface salinity (SSS) peaked at 50–60 ‰, levels too high for most shallow-water biota, such as zooxanthellate corals. Brachert et al. (2007) note that high salinity events, in both reefs and slope deposits, affected large areas of the Mediterranean but were not coupled with evaporative sea level drawdowns. This points to the potential existence of refugia for stenohaline organisms like *Halimeda*, allowing them to persist during periods of high salinity.

Before the Messinian Salinity Crisis (MSC), the Mediterranean region underwent significant environmental stress, severely affecting benthic ecosystems (Bosellini and Perrin, 2008; Vertino et al., 2014; Agiadi et al., 2024a,b). During the late Tortonian and early Messinian, coral reefs, especially in the western Mediterranean, were abundant but exhibited markedly reduced diversity, often dominated by just two genera, *Porites* and *Siderastrea* (Vertino et al., 2014). This environmental degradation near the onset of the MSC triggered a shift from coral frameworks to microbialite-dominated reefs, with *Halimeda* and vermetid gastropods becoming more prevalent (Brachert et al., 1996; Braga et al., 1996; Martin et al., 1997; Bosellini et al., 2002; Vescogni et al., 2008; Vertino et al., 2014). Stress on *Halimeda* and associated coral reefs intensified due to escalating changes in salinity, temperature, and nutrient availability. Reduced water exchange led to hypersaline conditions, with recorded SSS ranging from 48 to 58 ‰, well above the tolerance limits for most reef-associated organisms (Vasiliev et al., 2019). As the influx of Atlantic waters waned, oxygen-poor, hypersaline bottom waters developed, limiting vertical mixing, nutrient recycling, and biodiversity (Moissette et al., 2018; Agiadi et al., 2024a,b). Nutrient dynamics also shifted: reduced Atlantic inflow initially promoted productivity, but intensified water stratification limited nutrient cycling within the photic zone, diminishing primary productivity over time (Kontakiotis et al., 2022). Geochemical data from the Sorbas Basin, including $\delta^{13}C$ and δ^{1} O isotopes, further suggest that reduced freshwater input and increased aridity restricted nutrient availability (Reghizzi et al., 2017). Given this context, we believe internal waves (IWs) may have facilitated nutrient delivery to *Halimeda* bioherms, aiding their proliferation but also creating unfavorable conditions for coral reefs.

Temperature fluctuations further destabilized these ecosystems, with alternating cooling and warming phases, particularly from 6.4 to 6.1 million years ago (Kontakiotis et al., 2022). These adverse conditions contributed to episodic shifts within reef communities, with less tolerant corals being replaced by microbialites and *Halimeda* (Vertino et al., 2014). In areas such as Salento, Spain, and Crete, *Halimeda* bioherms exhibited thick aragonitic cements, potentially indicating high salinity stress (Brachert et al., 2007). Additionally, Vasiliev et al. (2019) noted Mediterranean SSS and SST oscillations, with a cooling phase around 6.4 million years ago followed by rapid warming near 6.15 million years ago, temporarily reducing salinity due to freshwater influxes, before returning to hypersaline conditions, which further stressed marine life.

The cumulative effects of tectonic isolation, nutrient limitations, salinity stress, and temperature fluctuations contributed to the decline of *Halimeda* bioherms and coral reefs, thereby preconditioning the Mediterranean for the extreme evaporitic phase of the MSC (Roveri et al., 2020; Bulian et al., 2023; Agiadi et al., 2024a,b). The presence of early cementation observed in *Halimeda* bioherms provides valuable insights into the interactions between biological activity, sedimentation, and environmental change during the Messinian.

6.2. Nutrients as the key factor on the blooming of Halimeda bioherms

The *Halimeda* bioherms of the Australian GBR have been extensively studied since the 1980s (Drew, 1983; Davies and Marshall, 1985; Drew and Abel, 1985; Orme, 1985; Drew and Abel, 1988; Roberts et al., 1987; Roberts et al., 1988; Hine et al., 1988; Marshall and Davies, 1988; Orme and Salama, 1988; Phipps and Roberts, 1988; Searle and Flood, 1988; McNeil et al., 2016, 2022).

Wolanski et al. (1988) outlined a direct relationship between the extensive distribution of *Halimeda* bioherms behind the GBR Ribbon Reefs and a stable supply of nutrients, that supports their persistence over time. McNeil et al. (2021a,b) further investigated this aspect by using the $^{15}N/^{14}N$ ratio ($\delta^{15}N$ skeletal organic material – SOM) on algal tissue. Although nutrients can originate from sources like terrestrial runoff, sewage input, or groundwater intrusion, the authors identified upwelling of cold water generated at great depths as a source of nutrient supply, specifically originating from thermocline waters (McNeil et al., 2021a,b).

The laterally and stratigraphically localized development of the Salento bioherms, suggests a periodic external nutrient input. As discussed earlier in the paragraph 6.1.1, we propose that this input gradually diminished due to the onset of the MSC, ultimately leading to the isolation of the Mediterranean Sea. According to Bosellini et al. (1999), the Salento carbonate system was part of an open, isolated platform, away from continental areas, characterized by a very limited freshwater influx and minimal terrigenous inputs. In contrast, the depositional setting of the Western Mediterranean localities, received significant amounts of freshwater and siliciclastic sediment, and were influenced by Atlantic waters (Esteban, 1979; Riding et al., 1991; Rouchy and Saint Martin, 1992; Martín and Braga, 1994; Franseen et al., 1998; Bourillot et al., 2009; Roveri et al., 2009, 2020; Pérez-Asensio et al., 2014). These differences suggest that the Salento carbonate system accounts for the smaller size of the *Halimeda* bioherms in Salento compared to those in Spain.

The availability of large quantities of nutrients is also attributed to specific climatic conditions, such as those found in tropical areas. Meteorological phenomena influenced the flourishing growth of *Halimeda*, as demonstrated by the large-scale bioherms of the Australian Great Barrier Reef (McNeil et al., 2021a,b), where local upwelling intrusions at the shelf-break likely intensified during peak El Niño periods, delivering more thermocline NO_3- toward *Halimeda* bioherms. This process is similarly inferred for the Oligocene bioherms present offshore of North Palawan – Philippines (Fournier et al., 2024), where upwelling currents associated with the onset of coastal jet in the Proto-South China Sea, established by a modern-like East Asian Monsoon summer circulation as early as the late Eocene, supplied essential nutrients for bioherm development. There is no evidence of meteorological phenomena of this kind, however, affecting the Mediterranean basin during the Messinian, and perhaps for this reason, the nutrients supplied to the bioherms in Salento were not sufficient for their development into large-size sedimentary bodies or their persistence.

6.2.1. Upwelling history in the central Mediterranean Basin

The upwelling of cold nutrient-rich waters is not unusual in the stratigraphic record of the central-eastern Mediterranean. Deposits associated with upwelling have been documented in various areas throughout the Tortonian (Fig. 12), including Malta (Föllmi et al., 2008), southeast Sicily (Föllmi et al., 2008), the Matese area in the central Appennines, the Maiella Mountain (Mutti and Bernoulli, 2003), the Latium-Abruzzi carbonate platform in the Appennines (Brandano et al., 2009), the Menorca Island and the Salento Peninsula (Föllmi et al., 2015; Brandano et al., 2016).

Specifically, the Salento Peninsula experienced a flooding during the Serravalian-Tortonian, which impacted the entire area. This event was responsible of the deposition of pelagic sediments of the Pietra Leccese inland and the Aturia Level hardground in coastal areas (Vescogni et al., 2018).

This Aturia Level is characterized by glauconitic and phosphoritic micrite, and rests between two thick, shallow-water formations: the Porto Badisco Calcarenites (Upper Oligocene) and the Novaglie Formation (Early Messinian), as can be observed in the Ciolo locality a few km north of the described sections, at the Ciolo locality (Fig. 1) (Föllmi et al., 2015). In this location, a small cave permits to observe a thin,

brownish layer a few tens of centimeters thick (Fig. 13). Moving southward, before the Tre Fratelli area, the Aturia Level reaching its maximum thickness of about 50 cm.

This regionally extensive condensed level, rich in macrofossils, has been related to a system of upwelling currents originating from the deepest areas of the Mediterranean Basin and reaching the eastern parts of the shelf (Föllmi et al., 2015). Changes in the direction and intensity of these bottom currents created a complex and variable depositional environment, where low sedimentation rates vertically alternate with areas of prevalent erosion (Vescogni et al., 2018).

Based on the occurrence of this hardground layer in the Salento Peninsula and other Mediterranean areas previously mentioned, which is interpreted as recording nutrient-rich upwelling currents throughout the Tortonian period, we infer that upwelling phenomena, persisted into the early Messinian. Although these phenomena were of lower intensity, they continued to supply the necessary nutrients for the development of the small *Halimeda* bioherms in the Salento Peninsula.

6.2.2. *Internal waves and their impact on nutrient dynamics*

An additional hydrodynamic mechanism to consider for the delivery of nutrients to the small bioherms of Salento is the potential action of internal waves (IWs) and tides. Internal waves and tides are gravity waves oscillations that occur within stratified ocean waters, propagating along the interfaces between layers of water with different densities (pycnocline) due to changes in temperature and salinity. These waves are generated by various forces, including tides, wind stress, storms etc. (Lamb, 2014; Boegman and Stastna, 2019; Woodson, 2018 and reference therein). Internal waves can travel over long distances and play a

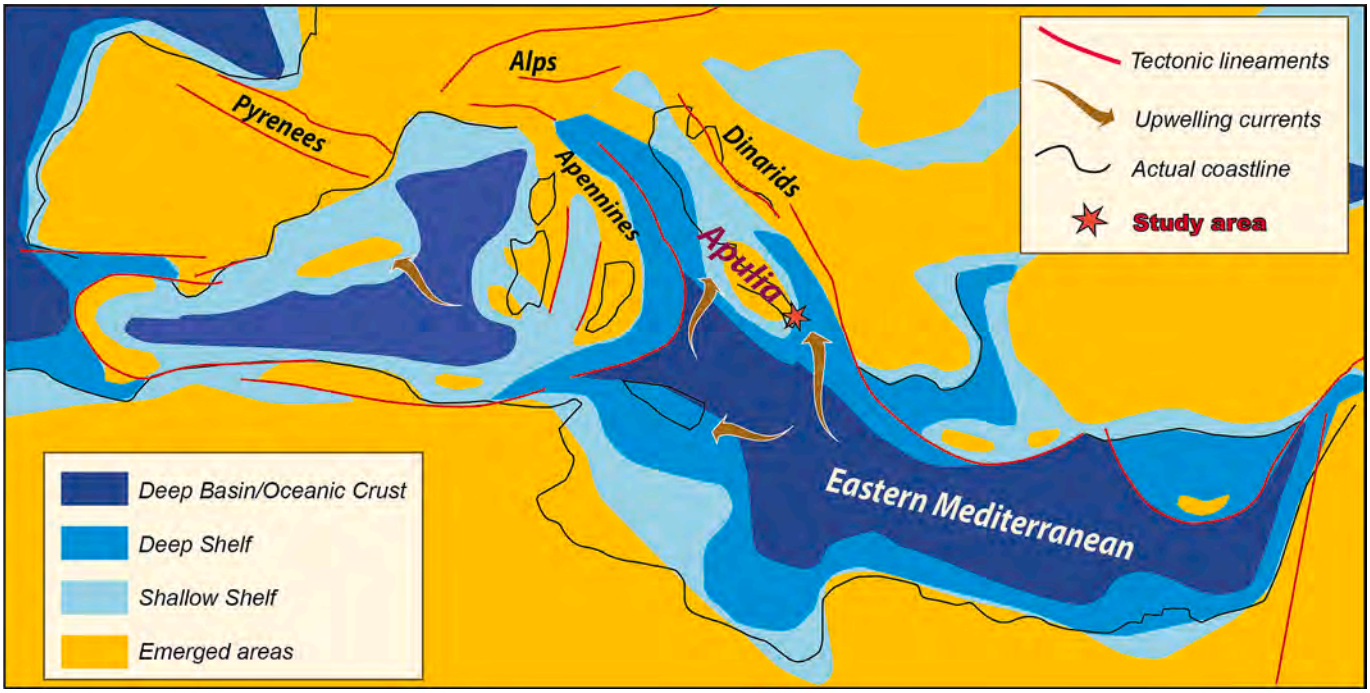

Fig. 12. Paleogeographic map of the Mediterranean area during the Tortonian - early Messinian with upwelling currents system that have promoted the formation of phosphatic condensed layers (modified after Popov et al., 2004). Considering the position of the Salento area and the proximity to the adjacent deep-water basin, we infer that weak upwelling currents were still active during the early Messinian.

Fig. 13. The condensed phosphatic hardground known as Aturia level (red line) located between the top of the Porto Badisco Formation and the base of the Novaglie Formation at the Ciolo locality with its characteristic brownish color. In the white box: specimen of *Aturia aturii*.

critical role in ocean mixing processes, transporting heat, nutrients, and larvae vertically through the water column (Leichter et al., 2005), as well as in sediment resuspension and transport, at various depth, along the continental slopes and platform where they breaks (Cacchione et al., 2002; Pomar et al., 2012; Lamb, 2014). IWs and internal tides can have significant impacts on the distribution of nutrients and the structure of marine ecosystems (Leichter et al., 2005; Pomar et al., 2012; Reid et al., 2019; Johnston and Colin, 2022).

It is not unusual for IWs to play a role in transporting nutrients to euphotic and mesophotic communities like corals and calcareous algae. It is known that in coastal regions, vertical mixing associated with IWs may result in a significant input of deep-water nutrients and particulate organic matter into shallow environments (Sandstrom and Elliott, 1984). Leichter et al. (1996) also documented that in modern Florida Keys, high excursions in temperature, salinity, current velocities, and concentration of chlorophyll-a are caused by the breaking of internal waves. Furthermore, Leichter et al. (1998, 2003, 2005) and Smith et al. (2004) reported enhanced growth rates of *Halimeda* specimen to be associated with enhanced fluxes of nutrients and suspended particles carried by internal waves. In addition, recent studies based on the nitrogen isotopic signature in the organic tissue of *Halimeda* segments in the GBR have confirmed a deep-water origin of the nutrients delivered to the *Halimeda* bioherms coming from the thermocline zone (McNeil et al., 2021a,b), where usually IWs are common.

While the essential role of nutrients in the development of many *Halimeda* species and bioherms in modern oceans is well-established (McNeil et al., 2021a,b), a recent study by Reolid et al. (2024) on *Halimeda* bioherms identified at Teagross Bank (Queensland Plateau – GBR) revealed a new type of bioherms. These bioherms, which are associated with mesophotic corals, are thought to have developed in an oligotrophic environment, and thus not related to upwelling currents. However, this work does not discuss the significance of the nutricline position (70–80 m), just below and near the depth of the bioherms (40–70 mbsl), where internal tides have been documented (Bendinger et al., 2023). In this context, without documented upwelling currents, internal tides can serve as a mechanism for transporting nutrients to this *Halimeda* communities. Moreover, their chlorophyll-a rate measurements are point-specific (<12 h) and therefore not representative of the significant seasonal variability, including phenomena such as tropical monsoons and storms that appear to favor the remixing of oceanic waters (Rao et al., 2018; McNeil et al., 2021a,b; Fournier et al., 2024).

In summary, internal waves (IWs) provide an additional mechanism for nutrient delivery to the small *Halimeda* bioherms examined in this study. This nutrient transport may be particularly significant in oligotrophic regions, where the absence or weakness of upwelling currents necessitates alternative nutrient enrichment mechanisms to support the growth of *Halimeda* bioherms in the mesophotic zone along the slope of the Novaglie Formation.

7. Conclusions

The detailed analysis and comparison of *Halimeda* bioherms in the "Tre Fratelli" and "Radar" sections, highlights their internal organization and depositional features. In the "Tre Fratelli" outcrop, the bioherm core is distinguished by in situ *Halimeda* segments alternating with rudstone and floatstone layers, while the upslope flank is characterized by thin to medium beds of rudstone and floatstone.

The small bioherms occur along the proximal-to-mid slope part of the Novaglie Formation. The internal organization and facies distribution of the "Tre Fratelli" bioherm are consistent with recent studies describing the internal structure of Holocene *Halimeda* mounds. Additionally, the presence of marine *syn*-depositional cements within the algal segments plays a critical role in preserving the internal structure of the algae and ensuring the stability of the deposits. These cements provide valuable insight into the fluctuations in salinity within the Mediterranean basin during the Messinian.

Comparison of lower Messinian *Halimeda* deposits in the Mediterranean area revealed that *Halimeda* bioherms development is limited to a few examples in Spain, southeastern Italy, and Crete Island. In contrast, *Halimeda*-rich beds have been reported across the Mediterranean region, including Morocco, Tunisia, and Egypt.

Nutrient supply is a crucial factor for the development of *Halimeda* bioherms. As observed in modern oceans, a stable supply of nutrients is essential for the persistence of these bioherms over time. Similarly, in the Salento area, sporadic and weak nutrient supply events could explain the development of these bioherms in a specific depositional setting along the mid slope, within a defined stratigraphic interval, just before the onset of Messinian Salinity Crisis. Hydrodynamic mechanisms such as the upwelling of nutrient-rich waters and internal waves may have facilitated the transport of nutrients to the bioherms.

Although the *Halimeda* bioherms in Salento are not as large as some modern analogs, they offer valuable insights into the sedimentary and paleoenvironmental dynamics of the central Mediterranean during the early Messinian. Recognizing *Halimeda* as a significant carbonate producer, particularly in mesophotic environments where other calcifying organisms are less productive, is crucial. In the context of global warming, *Halimeda* bioherms become increasingly important for their potential role in CO_2 sequestration. Further studies of both past and present bioherms are essential to understand their capacity to mitigate climate change impacts and possibly serve as refugia for other marine organisms, particularly in the mesophotic zone.

CRediT authorship contribution statement

Chiara Passaseo: Writing – review & editing, Writing – original draft, Methodology, Investigation, Formal analysis, Data curation. **Michele Morsilli:** Writing – review & editing, Supervision, Resources, Project administration, Methodology, Investigation, Funding acquisition, Formal analysis, Data curation, Conceptualization.

Declaration of competing interest

The authors declare that they have no known competing financial interests or personal relationships that could have appeared to influence the work reported in this paper.

Acknowledgements

We would like to sincerely thank Professor Alessandro Vescogni for sharing his expertise and knowledge about Salento outcrops and discussion in the field. This work was supported by funding from University of Ferrara (FAR 2021, 2022, 2023 - Morsilli; PhD funding - Passaseo).

We sincerely thank the editor and the two anonymous reviewers for their time and valuable insights, which significantly enhanced the clarity and quality of our work.

Data availability

Data will be made available on request.

References

Agiadi, K., Hohmann, N., Gliozzi, E., Thivaiou, D., Bosellini, F.R., Taviani, M., Bianucci, G., Collareta, A., Londeix, L., Faranda, C., Bulian, F., Koskeridou, E., Lozar, F., Mancini, A.M., Dominici, S., Moissette, P., Campos, I.B., Borghi, E., Iliopoulos, G., Antonarakou, A., Kontakiotis, G., Besiou, E., Zarkogiannis, S.D., Harzhauser, M., Sierro, F.J., Coll, M., Vasiliev, I., Camerlenghi, A., García-Castellanos, D., 2024a. The marine biodiversity impact of the Late Miocene Mediterranean salinity crisis. Science 385, 986–991.

Agiadi, K., Hohmann, N., Gliozzi, E., Thivaiou, D., Bosellini, F.R., Taviani, M., Bianucci, G., Collareta, A., Londeix, L., Faranda, C., Bulian, F., Koskeridou, E., Lozar, F., Mancini, A.M., Dominici, S., Moissette, P., Campos, I.B., Borghi, E., Iliopoulos, G., Antonarakou, A., Kontakiotis, G., Besiou, E., Zarkogiannis, S.D., Harzhauser, M., Sierro, F.J., Coll, M., Vasiliev, I., Camerlenghi, A., García-

Castellanos, D., 2024b. Late Miocene transformation of Mediterranean Sea biodiversity. Science Advances 10, 1–12.
Bendinger, A., Cravatte, S., Gourdeau, L., Brodeau, L., Albert, A., Tchilibou, M., Lyard, F., Vic, C., 2023. Regional modeling of internal-tide dynamics around New Caledonia-part 1: coherent internal-tide characteristics and sea surface height signature. Ocean Science 19, 1315–1338.
Bernoulli, D., 2001. Mesozoic–tertiary carbonate platforms, slopes and basins ofthe external Apennines and Sicily. In: Vai, G.B., Martini, I.P. (Eds.), Anatomy of an Orogen: The Apennines and Adjacent Mediterranean Basins. Kluwer Acad. Publishers, pp. 307–325.
Boegman, L., Stastna, M., 2019. Sediment resuspension and transport by internal solitary waves. Annual Review of Fluid Mechanics 51, 129–154.
Bosellini, A., Bosellini, F.R., Colalongo, M.L., Parente, M., Russo, A., Vescogni, A., 1999. Stratigraphic architecture of the salento coast from capo d'otranto to S. Maria Di Leuca (Apulia, Southern Italy). Rivista Italiana di Paleontologia e Stratigrafia 105, 397–416.
Bosellini, F.R., 2006. Biotic changes and their control on Oligocene-Miocene reefs: a case study from the Apulia Platform margin (southern Italy). Palaeogeography Palaeoclimatology Palaeoecology 241, 393–409.
Bosellini, F.R., Perrin, C., 2008. Estimating Mediterranean Oligocene–Miocene sea-surface temperatures: an approach based on coral taxonomic richness. Palaeogeography Palaeoclimatology Palaeoecology 258, 71–88.
Bosellini, F.R., Russo, A., 1992. Stratigraphy and facies of an oligocene fringing reef (Castro Limestone, Salento Peninsula, Southern Italy). Facies 26, 145–165.
Bosellini, F.R., Russo, A., Vescogni, A., 2001. Messinian reef-building assemblages of the Salento Peninsula (southern Italy): Palaeobathymetric and palaeoclimatic significance. Palaeogeography Palaeoclimatology Palaeoecology 175, 7–26.
Bosellini, F.R., Russo, A., Vescogni, A., 2002. The Messinian reef complex of the Salento Peninsula (southern Italy): stratigraphy, facies and paleoenvironmental interpretation. Facies 47, 91–112.
Bossio, A., Mazzei, R., Monteforti, B., Salvatorini, G., 1994. La successione miocenica nell'area tipo delle Calcareniti di Andrano (Puglia, Italia meridionale). Bollettino della Societa Paleontologica Italiana 33, 249–255.
Bourillot, R., Vennin, E., Rouchy, J.M., Durlet, C., Rommevaux, V., Kolodka, C., Knap, F., 2009. Structure and evolution of a Messinian mixed carbonate-siliciclastic platform: the role of evaporites (Sorbas Basin, South-east Spain). Sedimentology 57, 477–512.
Brachert, T.C., Betzler, C., Braga, J.C., Martin, J.M., 1996. Record of climatic change in neritic carbonates: turnover in biogenic associations and depositional modes (Late Miocene, southern Spain). Geologische Rundschau 85, 327–337.
Brachert, T.C., Vescogni, A., Bosellini, F.R., Reuter, M., Mertz-Kraus, R., 2007. High salinity variability during the early Messinian revealed by stable isotope signatures from vermetid and *Halimeda* reefs of the Mediterranean region. Geologica Romana 40, 51–66.
Braga, J.C., Martín, J.M., 1996. Geometries of reef advance in response to relative sea-level changes in a Messinian (uppermost Miocene) fringing reef (Cariatiz reef, Sorbas Basin, SE Spain). Sedimentary Geology 107, 61–81.
Braga, J.C., Martín, J.M., Riding, R., 1996. Internal structure of segment reefs: *Halimeda* algal mounds in the Mediterranean Miocene. Geology 24, 35–38.
Brandano, M., Mateu-Vicens, G., Gianfagna, A., Corda, L., Billi, A., Quaresima, S., Simonetti, A., 2009. Hardground development and drowning of a Miocene carbonate ramp (Latium-Abruzzi): from tectonic to paleoclimate. Journal of Mediterranean Earth Sciences 1, 47–56.
Brandano, M., Westphal, H., Mateu-Vicens, G., Preto, N., Obrador, A., 2016. Ancient upwelling record in a phosphate hardground (Tortonian of Menorca, Balearic Islands, Spain). Marine and Petroleum Geology 78, 593–605.
Bulian, F., Jiménez-Espejo, F.J., Andersen, N., Larrasoaña, J.C., Sierro, F.J., 2023. Mediterranean water in the Atlantic Iberian margin reveals early isolation events during the Messinian Salinity Crisis. Global and Planetary Change 231, 104297.
Cacchione, D.A., Pratson, L.F., Ogston, A.S., 2002. The shaping of continental slopes by internal tides. Science 296, 724–727.
Castro-Sanguino, C., Bozec, Y., Mumby, P., 2020. Dynamics of carbonate sediment production by *Halimeda*: implications for reef carbonate budgets. Marine Ecology Progress Series 639, 91–106.
Cestari, R., Sirna, G., 1987. Rudist fauna in the Maastrichtian deposits of southern Salento (Southern Italy). Memorie della Società Geologica Italiana 40, 133–147.
Conard, M., Rioult, M., 1977. *Halimeda elliotti* nov. sp., Algue calcaire (Chlorophyceae) du Turonien des Alpes-Maritimes (SE France). Géologie Méditerranéenne 4, 83–97.
Cornée, J.J., Saint Martin, J.P., Conesa, G., André, J.P., Muller, J., Benmoussa, A., 1996. Anatomie de quelques platesformes carbonatées progradantes messiniennes de Méditerranée occidentale. Bulletin de la Societe Geologique de France 167, 495–507.
Cornée, J.J., Saint Martin, J.P., Conesa, G., Münch, P., André, J.P., Saint Martin, S., Roger, S., 2004. Correlations and sequence stratigraphic model for Messinian carbonate platforms of the western and central Mediterranean. International Journal of Earth Sciences 93, 621–633.
Cunningham, K.J., Collins, L.S., 2002. Controls on facies and sequence stratigraphy of an upper Miocene carbonate ramp and platform, Melilla basin, NE Morocco. Sedimentary Geology 146, 285–304.
Davies, P.J., Marshall, J.F., 1985. *Halimeda* bioherms – low energy reefs, northern Great Barrier Reef. In: Proc. 5th Int. Coral Reef Symp, 5, pp. 1–7.
Dragastan, O.N., Herbig, H.G., 2007. *Halimeda* (green siphonous algae) from the Paleogene of (Morocco) - taxonomy, phylogeny and paleoenvironment. Micropaleontology 53, 1–72.
Dragastan, O.N., Soliman, H.A., 2002. Paleogene calcareous algae from Egypt. Micropaleontology 48, 1–30.
Drew, E.A., 1983. *Halimeda* biomass, growth rates and sediment generation on reefs in the central Great Barrier Reef Province. Coral Reefs 2, 101–110.
Drew, E.A., 1993. Production of geological structures by the green alga *Halimeda*. South Pacific Underwater Medicine Society 23, 93–102.
Drew, E.A., Abel, K.M., 1985. Biology, sedimentology, and geography of the vast inter-reefal *Halimeda* meadows within the Great Barrier Reef province. In: Proc. 5th Int. Coral Reef Symp, 5, pp. 15–20.
Drew, E.A., Abel, K.M., 1988. Studies on *Halimeda* - I. The distribution and species composition of *Halimeda* meadows throughout the Great Barrier Reef Province. Coral Reefs 6, 195–205.
Dunham, R.J., 1962. Classification of carbonate rocks according to depositional textures. In: Ham, W.E. (Ed.), Classification of Carbonate Rocks, a Symposium, AAPG Memoir n. 1, pp. 108–121.
Elliott, G.F., 1959. Fossil calcareous algal floras of the Middle East with a note on a Cretaceous problematicum, gen. et sp. Nov. Quarterly Journal of the Geological Society of London 115, 217–232.
Embry, A.F., Klovan, J.E., 1971. A Late Devonian reef tract on northeastern Banks Island, NWT. Bulletin of Canadian Petroleum Geology 19, 730–781.
Esteban, M., 1979. Significance of the upper Miocene coral reefs of the Western Mediterranean. Palaeogeography Palaeoclimatology Palaeoecology 29, 169–188.
Föllmi, K.B., Gertsch, B., Renevey, J.P., de Kaenel, E., Stille, P., 2008. Stratigraphy and sedimentology of phosphate-rich sediments in Malta and southeastern Sicily (latest Oligocene to early Late Miocene). Sedimentology 55, 1029–1051.
Föllmi, K.B., Hofmann, H., Chiaradia, M., de Kaenel, E., Frijia, G., Parente, M., 2015. Miocene phosphate-rich sediments in Salento (southern Italy). Sedimentary Geology 327, 55–71.
Fornos, J.J., Forteza, V., Jaume, C., Martinez-Taberner, A., 1992. Present-day *Halimeda* carbonate sediments in temperate mediterranean embayments: Fornells, Balearic Islands. Sedimentary Geology 75, 283–293.
Fournier, F., Teillet, T., Licht, A., Borgomano, J., Montaggioni, L., 2024. Eocene-Oligocene large-scale circulation of the East Asian summer monsoon recorded in neritic carbonates of the proto-South China Sea. Palaeogeography Palaeoclimatology Palaeoecology 633 doi:111883.10.1016/j.palaeo.2023.111883.
Franseen, E.K., Mankiewicz, C., 1991. Depositional sequences and correlation of middle (?) to late Miocene carbonate complexes, Las Negras and Nijar areas, southeastern Spain. Sedimentology 38, 871–898.
Franseen, E.K., Goldstein, R.H., Farr, M.R., 1998. Quantitative controls on location and architecture of carbonate depositional sequences: Upper Miocene, Cabo de Gata region, SE Spain. Journal of Sedimentary Research 68, 283–298.
Ghosh, A.K., Chakraborty, A., Mazumder, A., 2017. *Halimeda* bioherms from the Serravallian (MiddleMiocene) of Little Andaman Island, India. Micropaleontology 63, 67–75.
Hillis, L., 1997. Coralgal reefs from a calcareous green alga perspective and a first carbonate budget. In: Proceedings of 8th International Coral Reef Symposium, 1, pp. 761–766.
Hillis-Colinvaux, L., 1980. Ecology and taxonomy of *Halimeda*: primary producer of coral reefs. Advances in Marine Biology 17, 327.
Hillis-Colinvaux, L., 1986. Deep water populations of Halimeda in the economy of an atoll. Bulletin of Marine Science 38, 155–169.
Hine, A.C., Hallock, P., Harris, M.W., Mullins, H.T., Belknap, D.F., Jaap, W.C., 1988. *Halimeda* bioherms along an open seaway: Miskito Channel, Nicaraguan Rise, SW Caribbean Sea. Coral Reefs 6, 173–178.
Insalaco, E., 1998. The descriptive nomenclature and classification of growth fabrics in fossil scleractinian reefs. Sedimentary Geology 118, 159–186.
Johnston, T.M.S., Colin, P.L., 2022. Upwelling and downwelling driven by the north equatorial countercurrent and internal waves at Hatohobei Island and Helen Reef, Palau. Journal of Geophysical Research, Oceans 127, 1–18.
Kontakiotis, G., Butiseacă, G.A., Antonarakou, A., Agiadi, K., Zarkogiannis, S.D., Krsnik, E., Besiou, E., Zachariasse, W.J., Lourens, L., Thivaiou, D., Koskeridou, E., Moissette, P., Mulch, A., Karakitsios, V., Vasiliev, I., 2022. Hypersalinity accompanies tectonic restriction in the eastern Mediterranean prior to the Messinian Salinity Crisis. Palaeogeography Palaeoclimatology Palaeoecology 592, 110903.
Lamb, K.G., 2014. Internal wave breaking and dissipation mechanisms on the continental slope/shelf. Annual Review of Fluid Mechanics 46, 231–254.
Laviano, A., 1996. Late Cretaceous rudist assemblages from the Salento peninsula (southern Italy). Geologica Romana 32, 1–14.
Leichter, J.J., Shellenbarger, G., Genovese, S.J., Wing, S.R., 1998. Breaking internal waves on a Florida (USA) coral reef: a plankton pump at work? Marine Ecology Progress Series 166, 83–97.
Leichter, J.J., Stewart, H.L., Miller, S.L., 2003. Episodic nutrient transport to Florida coral reefs. Limnology and Oceanography 48, 394–1407.
Leichter, J.J., Deane, G.B., Stokes, M.D., 2005. Spatial and temporal variability of internal wave forcing on a coral reef. Journal of Physical Oceanography 35, 1945–1962.
Leichter, J.J., Wing, S.R., Miller, S.L., Denny, M.W., 1996. Pulsed delivery of subthermocline water to Conch Reef (Florida Keys) by internal tidal bores. Limnology and Oceanography 41, 1490–1501.
Littler, M.M., Littler, D.S., Blair, S.M., Norris, J.N., 1985. Deepest known plant life discovered on an uncharted seamount. Science 227, 57–59.
Mankiewicz, C., 1988. Coral Reefs Occurrence and paleoecologic significance of *Halimeda* in late Miocene reefs, southeastern Spain. Coral Reefs 6, 271–279.
Mann, T., Wizemann, A., Stuhr, M., Kappelmann, Y., Janßen, A., Jompa, J., Westphal, H., 2022. Shallow-marine carbonate cementation in Holocene segments of the calcifying green alga *Halimeda*. Sedimentology 69, 282–300.
Marshall, J.F., Davies, P.J., 1988. *Halimeda* bioherms of the northern Great Barrier Reef. Coral Reefs 6, 139–148.

Martín, J.M., Braga, J.C., 1994. Messinian events in the Sorbas Basin in southeastern Spain and their implications in the recent history of the Mediterranean. Sedimentary Geology 90, 257–268.
Martin, J.M., Braga, J.C., Riding, R., 1997. Late Miocene *Halimeda* algal-microbial segment reef in the marginal Mediterranean Sorbas Basin, Spain. Sedimentology 44, 441–456.
Martinis, B., 1962. Lineamenti strutturali della parte meridionale della Penisola Salentina. Geologica Romana 1, 11–23.
McNeil, M.A., Webster, J.M., Beaman, R.J., Graham, T.L., 2016. New constraints on the spatial distribution and morphology of the *Halimeda* bioherms of the Great Barrier Reef, Australia. Coral Reefs 35, 1343–1355.
McNeil, M.A., Nothdurft, L., Erler, D., Hua, Q., Webster, J.M., 2021a. Variations in Mid- to Late Holocene Nitrogen Supply to Northern Great Barrier Reef *Halimeda* Macroalgal Bioherms. Paleoceanography and Paleoclimatology 36, 1–18.
McNeil, M.A., Nothdurft, L.D., Dyriw, N.J., Webster, J.M., Beaman, R.J., 2021b. Morphotype differentiation in the Great Barrier Reef *Halimeda* bioherm carbonate factory: internal architecture and surface geomorphometrics. Depositional Record 7, 176–199.
McNeil, M.A., Nothdurft, L.D., Hua, Q., Webster, J.M., Moss, P., 2022. Evolution of the inter-reef *Halimeda* carbonate factory in response to Holocene sea-level and environmental change in the Great Barrier Reef. Quaternary Science Reviews 277, 107347.
Milliman, J., 1993. Production and accumulation of calcium carbonate in the ocean: budget of a nonsteady state. Global Biogeochemical Cycles 7, 927–957.
Moissette, P., Cornée, J.J., Antonarakou, A., Kontakiotis, G., Drinia, H., Koskeridou, E., Tsourou, T., Agiadi, K., Karakitsios, V., 2018. Palaeoenvironmental changes at the Tortonian/Messinian boundary: a deep-sea sedimentary record of the eastern Mediterranean Sea. Palaeogeography Palaeoclimatology Palaeoecology 505, 217–233.
Morsilli, M., Hairabian, A., Borgomano, J., Nardon, S., Adams, E., Gartner, G.B., 2017. The Apulia Carbonate Platform-Gargano Promontory, Italy (Upper Jurassic-Eocene). American Association of Petroleum Geologists Bulletin 101, 523–531.
Morsilli, M., Hairabian, A., Borgomano, J., Nardon, S., Adams, E., Bracco Gartner, G., 2021. A journey along the Gargano Promontory (Southern Italy): The Late Jurassic to Eocene Apulia Carbonate Platform evolution. In: Wright, V.P., Della Porta, G. (Eds.), Field Guides to Exceptionally Exposed Carbonate Outcrops. International Association of Sedimentologists, pp. 395–480.
Multer, H.G., 1988. Growth rate, ultrastructure and sediment contribution of *Halimeda incrassata* and *Halimeda monile*, Nonsuch and Falmouth Bays, Antigua, W.I. Coral Reefs 6, 179–186.
Münch, P., Roger, S., Cornée, J.J., Saint Martin, J.P., Féraud, G., Moussa, A. Ben, 2001. Restriciton des communications entre l'Atlantique et la Méditerranée au Messinien: Apport de la téphrochronologie dans la plateforme carbonatée et le bassin de Mellilla-Nador (Rif nord-oriental, Maroc). Comptes Rendus de l'Academie de Sciences - Serie IIa: Sciences de la Terre et des Planetes 332, 569–576.
Muntaner-Gonzalez, C., Martin-Abadal, M., Gonzalez-Cid, Y., 2024. A deep learning approach to estimate *Halimeda incrassata* invasive stage in the Mediterranean Sea. Journal of Marine Science and Engineering 12, 1–20.
Mutti, M., Bernoulli, D., 2003. Early marine lithification and hardground development on a Miocene ramp (Maiella, Italy): key surfaces to track changes in trophic resources in non-topical carbonate settings. Journal of Sedimentary Research 73, 296–308.
Nardin, M., Rossi, D., 1966. Condizioni strutturali della zona compresa nel Foglio Otranto (Provincia di Lecce). Museo Civico di Storia Naturale Verona 14, 415–430.
Orme, G.R., Salama, M.S., 1988. Form and seismic stratigraphy of *Halimeda* banks in part of the northern Great Barrier Reef Province. Coral Reefs 6, 131–137.
Orme, R., 1985. The sedimentological importance of *Halimeda* in the development of back-reef lithofacies, northern Great Barrier Reef (Australia). In: Proc. 5th Int. Coral Reef Symp, 5, pp. 31–37.
Orme, R., Riding, R., 1995. *Halimeda* Segment Reefs of the Northern Great Barrier Reef. In: British Sedimentological Research Group, Annu. Meet. Abstr. Durham, p. 64.
Parente, M., 1994. A revised stratigraphy of the Upper Cretaceous to Oligocene units from southeastern Salento (Apulia, southern Italy). Bollettino della Societa Paleontologica Italiana 33, 155–170.
Passaseo, C., Morsilli, M., 2024. *Halimeda*-rich beds in a mixed carbonate system from a pre-evaporitic Messinian reef (Crete Island, Greece). In: AAPG Cross Regional Carbonates and Mixed Carbonate Systems Symposium, Palermo, p. 82.
Pérez-Asensio, J.N., Aguirre, J., Schmiedl, G., Civis, J., 2014. Messinian productivity changes in the northeastern Atlantic and their relationship to the closure of the Atlantic-Mediterranean gateway: implications for Neogene palaeoclimate and palaeoceanography. Journal of the Geological Society of London 171, 389–400.
Perry, C.T., Morgan, K.M., Salter, M.A., 2016. Sediment generation by *Halimeda* on atoll interior coral reefs of the southern Maldives: a census-based approach for estimating carbonate production by calcareous green algae. Sedimentary Geology 346, 17–24.
Phipps, C.V.G., Roberts, H.H., 1988. Seismic characteristics and accretion history of *Halimeda* bioherms on Kalukalukuang Bank, eastern Java Sea (Indonesia). Coral Reefs 6, 149–159.
Pomar, L., Morsilli, M., Hallock, P., Bádenas, B., 2012. Internal waves, an under-explored source of turbulence events in the sedimentary record. Earth-Science Reviews 111, 56–81.
Pomar, L., Mateu-Vicens, G., Morsilli, M., Brandano, M., 2014. Carbonate ramp evolution during the Late Oligocene (Chattian), Salento Peninsula, southern Italy. Palaeogeography Palaeoclimatology Palaeoecology 404, 109–132.
Poncet, J., 1989. Présence du genre *Halimeda* Lamouroux, 1812 (algue verte calcaire) dans le Permien supérieur du Sud Tunisien. Revue de Micropaleontologie 32, 40–44.
Popov, S.V., Rögl, F., Rozanov, A.Y., Steininger, F.F., Shcherba, I.G., Kovac, M., 2004. Lithological-paleogoegraphic maps of Paratethys. Courier Forschungsinstitut Senckenberg 250, 46.
Rao, V.P., Veerayya, M., Nair, R.R., Dupeuble, P.A., Lamboy, M., 1994. Late Quaternary *Halimeda* bioherms and aragonitic faecal pellet-dominated sediments on the carbonate platform of the western continental shelf of India. Marine Geology 121, 293–315.
Rao, V.P., Mahale, V.P., Chakraborty, B., 2018. Bathymetry and sediments on the carbonate platform off western India: significance of *Halimeda* bioherms in carbonate sedimentation. Journal of Earth System Science 127, 1–16.
Rees, S.A., 2006. Coral Reefs of the Indo-Pacific and Changes in Global Holocene Climate. PhD thesis. University of Southampton, UK, p. 188.
Rees, S.A., Opdyke, B.N., Wilson, P.A., Henstock, T.J., 2007. Significance of *Halimeda* bioherms to the global carbonate budget based on a geological sediment budget for the Northern Great Barrier Reef, Australia. Coral Reefs 26, 177–188.
Reghizzi, M., Gennari, R., Douville, E., Lugli, S., Manzi, V., Montagna, P., Roveri, M., Sierro, F.J., Taviani, M., 2017. Isotope stratigraphy (87Sr/86Sr, δ18O, δ13C) of the Sorbas basin (Betic Cordillera, Spain): paleoceanographic evolution across the onset of the Messinian salinity crisis. Palaeogeography Palaeoclimatology Palaeoecology 469, 60–73.
Reid, E.C., De Carlo, T.M., Cohen, A.L., Wong, G.T.F., Lentz, S.J., Safaie, A., Hall, A., Davis, K.A., 2019. Internal waves influence the thermal and nutrient environment on a shallow coral reef. Limnology and Oceanography 64, 1949–1965.
Reolid, J., Betzler, C., Braga, J.C., Martín, J.M., Lindhorst, S., Reijmer, J.J.G., 2014. Reef slope geometries and facies distribution: controlling factors (Messinian, SE Spain). Facies 60, 737–753.
Reolid, J., Bialik, O.M., Lindhorst, S., Eisermann, J.O., Petrovic, A., Hincke, C., Beaman, R.J., Webster, J.M., Betzler, C., 2024. A new type of *Halimeda* bioherm on the Queensland Plateau, NE Australia. Coral Reefs 43, 801–821.
Riding, R., Martín, J.M., Braga, J.C., 1991. Coral-stromatolite reef framework, Upper Miocene, Almería, Spain. Sedimentology 38, 799–818.
Ries, J.B., Cohen, A.L., McCorkle, D.C., 2009. Marine calcifiers exhibit mixed responses to CO2-induced ocean acidification. Geology 37, 1131–1134.
Roberts, H.H., Aharon, C.V., Phipps, P., 1988. Morphology and sedimentology of *Halimeda* bioherms from the eastern Java Sea (Indonesia). Coral Reefs 6, 161–172.
Roberts, H.H., Phipps, C.V., Effendi, L., 1987. *Halimeda* bioherms of the eastern Java Sea, Indonesia. Geology 15, 371–374.
Roger, S., Munch, P.H., Cornée, J.J., Saint Martin, J.P., Féraud, G., Conesa, G., Pestrea, S., Ben Moussa, A., 2000. 40Ar/39Ar dating of the pre-evaporitic Messinian marine sequences of the Melilla basin (Morocco): a proposal for some biosedimentary events as isochrons around the Alboran Sea. Earth and Planetary Science Letters 179, 101–113.
Rouchy, J.M., Saint Martin, J.P., 1992. Late Miocene events in the Mediterranean as recorded by carbonate-evaporite relations. Geology 20, 629–632.
Roveri, M., Gennari, R., Lugli, S., Manzi, V., 2009. The Terminal Carbonate Complex: the record of sea-level changes during the Messinian salinity crisis. GeoActa 8, 63–77.
Roveri, M., Lugli, S., Manzi, V., Reghizzi, M., Rossi, F.P., 2020. Stratigraphic relationships between shallow-water carbonates and primary gypsum: insights from the Messinian succession of the Sorbas Basin (Betic Cordillera, Southern Spain). Sedimentary Geolology 404, 105–678.
Saint Martin, J.P., Cornée, J.J., 1996. The Messinian reef complex of Melilla, northeastern Rif, Morocco: models for carbonate stratigraphy from Miocene reef complexes of Mediterranean regions. In: SEPM Concepts in Sedimentology and Paleontology, 5, pp. 227–237.
Saint Martin, J.P., Cornee, J.J., Conesa, G., Bessedik, M., Belkebir, L., Mansour, B., Moisette, P., Anglada, R., 1992. Un dispositif particulier de plateforme carbonatée messinienne: la bordure meridionale du bassin du Bas-Chelif Algerie. Comptes Rendus de l'Academie des Sciences Serie II 315, 1365–1372.
Sandstrom, H., Elliott, J.A., 1984. Internal tidae and solitons on the Scotian shelf: a nutrient pump at work. Journal of Geophysical Research 89, 6415–6426.
Sarkar, S., Singh, Y.P., Verma, P., 2024. Paleoecological and paleobiogeographic implications of a seagrass-indicating foralgal skeletal assemblage: retracing the Burdigalian Quilon Limestone (Kerala Basin, SW India). Marine Micropaleontology 187, 102–330.
Searle, D.F., Flood, P.G., 1988. *Halimeda* bioherms of the Swains reefs – southern Great Barrier Reef. In: 6th International Coral Reef Symposium, 3, pp. 139–144.
Smith, J.E., Smith, C.M., Vroom, P.S., Beach, K.L., Miller, S., Buckley, J., Cooper, C., Rutten, O., Smith, M., Lounsbury, R., Florrent, M., Styron, J., Dunbar, T., Hulsbeck, M., Kessling, D., 2004. Nutrient and growth dynamics of *Halimeda tuna* on Conch Reef, Florida Keys: possible influence of internal tides on nutrient status and physiology immense support of the entire NURC staff, including. Limnology and Oceanography 49, 1923–1936.
Stanley, S.M., Ries, J.B., Hardie, L.A., 2010. Increasing production of calcite and slower growth for the major sediment-producing alga *Halimeda* as the Mg/Ca ratio of seawater is lowered to a "calcite sea" level. Journal of Sedimentary Research 80, 6–16.
Stokes, M.D., Leichter, J.J., Wing, S.R., 2020. Spatial variations in the stable isotope composition of the benthic algae, *Halimeda tuna*, and implications for paleothermometry. Scientific Reports 10, 1–14.
Takayanagi, H., Iryu, Y., Yamada, T., Oda, M., Yamamoto, K., Sato, T., Chiyonobu, S., Nishimura, A., Nakazawa, T., Shiokawa, S., 2007. Carbonate deposits on submerged seamounts in the northwestern Pacific Ocean. Island Arc 16, 394–419.
Tozzi, M., 1993. Assetto tettonico dell'Avampaese Apulo meridionale (Murge meridionali - Salento) sulla base dei dati strutturali. Geologica Romana 29, 95-11.
Tropeano, M., Spalluto, L., Meloni, D., Moretti, M., Sabato, L., 2022. 'Isolated base-of-slope aprons': an oxymoron for shallow-marine fan-shaped, temperate-water,

carbonate bodies along the south-east Salento escarpment (Pleistocene, Apulia, southern Italy). Sedimentology 69, 345–371.
Vasiliev, I., Karakitsios, V., Bouloubassi, I., Agiadi, K., Kontakiotis, G., Antonarakou, A., Triantaphyllou, M., Gogou, A., Kafousia, N., de Rafélis, M., Zarkogiannis, S., Kaczmar, F., Parinos, C., Pasadakis, N., 2019. Large sea surface temperature, salinity, and productivity-preservation changes preceding the onset of the Messinian Salinity Crisis in the Eastern Mediterranean Sea. Paleoceanography and Paleoclimatology 34, 182–202.
Vertino, A., Stolarski, J., Bosellini, F.R., Taviani, M., 2014. Mediterranean Corals Through Time: From Miocene to Present, the Mediterranean Sea: Its History and Present Challenges. Springer Netherlands, Dordrecht.
Vescogni, A., 2000. Evoluzione delle costruzioni a vermetidi e loro utilizzo come "markers" paleobatimetrici e paleoclimatici. Giornale di Geologia 62, 55–61.
Vescogni, A., Bosellini, F.R., Reuter, M., Brachert, T.C., 2008. Vermetid reefs and their use as palaeobathymetric markers: new insights from the Late Miocene of the Mediterranean (Southern Italy, Crete). Palaeogeography Palaeoclimatology Palaeoecology 267, 89–101.
Vescogni, A., Bosellini, F.R., Cipriani, A., Gürler, G., Ilgar, A., Paganelli, E., 2014. The Dağpazarı carbonate platform (Mut Basin, Southern Turkey): facies and environmental reconstruction of a coral reef system during the Middle Miocene Climatic Optimum. Palaeogeography Palaeoclimatology Palaeoecology 410, 213–232.
Vescogni, A., Vertino, A., Bosellini, F.R., Harzhauser, M., Mandic, O., 2018. New paleoenvironmental insights on the Miocene condensed phosphatic layer of Salento (southern Italy) unlocked by the coral-mollusc fossil archive. Facies 64, 7. https://doi.org/10.1007/s10347-018-0520-9.
Vescogni, A., Guido, A., Cipriani, A., Gennari, R., Lugli, F., Lugli, S., Manzi, V., Reghizzi, M., Roveri, M., 2022. Palaeoenvironmental setting and depositional model of upper Messinian microbialites of the Salento Peninsula (Southern Italy): a central Mediterranean Terminal Carbonate Complex. Palaeogeography Palaeoclimatology Palaeoecology 595, 110970.
Wei, Z., Zhang, Y., Yang, F., Long, L., 2022. Diurnal fluctuations in seawater pCO2 amplify the negative effects of ocean acidification on the biotic performance of the calcifying macroalga *Halimeda opuntia*. Frontiers in Marine Science 9, 1–14.
Wilbur, K.M., Hillis-Colinvaux, L., Watabe, N., 1969. Electron microscope study of calcification in the alga *Halimeda* (Order Siphonales). Phycologia 8, 27–35.
Wizemann, A., Meyer, F.W., Westphal, H., 2014. A new model for the calcification of the green macro-alga *Halimeda opuntia* (Lamouroux). Coral Reefs 33, 951–964.
Wolanski, E., Drew, E., Abel, K.M., O'Brien, J., 1988. Tidal jets, nutrient upwelling, and their influence on the productivity of the alga *Halimeda* in the Ribbon Reefs, Great Barrier Reef. Estuarine, Coastal and Shelf Science 26, 169–201.
Woodson, C.B., 2018. The fate and impact of internal waves in nearshore ecosystems. Annual Review of Marine Science 10, 421–441.
Xu, H., Zhao, X., Eberli, G.P., Liu, X., Zhu, Y., Cai, Y., Luo, W., Yan, G., Zhang, B., Wei, K., Shi, J., 2015. Biogenic carbonate formation and sedimentation in the Xisha Islands: evidences from living *Halimeda*. Acta Oceanologica Sinica 34, 62–73.